



TALLINN UNIVERSITY OF TECHNOLOGY

SCHOOL OF ENGINEERING

Department of Electrical Power Engineering and Mechatronics

DEVELOPMENT OF A WHEEL TEST BENCH WITH ITS ASSOCIATED DIGITAL TWIN

RATTA KATSESTENDI VÄLJATÖÖTAMINE KOOS SELLEGA SEOTUD DIGITAALSE KAKSIKUGA

MASTER THESIS

Student: Robin Köppe

Student code: 241398MAHM

Supervisor: Mahmoud Ibrahim Hassanin
Mohamed, Early Stage Researcher

Co-supervisor: Anton Rassõlkin, Tenured Associate
Professor

Tallinn 2024

AUTHOR'S DECLARATION

Hereby I declare, that I have written this thesis independently.

No academic degree has been applied for based on this material. All works, major viewpoints and data of the other authors used in this thesis have been referenced.

"13" May 2024

Author:

/signature /

Thesis is in accordance with terms and requirements

"....." 2024

Supervisor:

/signature/

Accepted for defence

"....." 2024

Chairman of theses defence commission:

/name and signature/

Non-exclusive licence for reproduction and publication of a graduation thesis¹

I, Robin Köppe

1. grant Tallinn University of Technology free licence (non-exclusive licence) for my thesis "Development of a test bench for wheels of a propulsion drive system including the associated digital twin",

supervised by Mahmoud Ibrahim Hassanin Mohamed,

1.1 to be reproduced for the purposes of preservation and electronic publication of the graduation thesis, incl. to be entered in the digital collection of the library of Tallinn University of Technology until expiry of the term of copyright;

1.2 to be published via the web of Tallinn University of Technology, incl. to be entered in the digital collection of the library of Tallinn University of Technology until expiry of the term of copyright.

2. I am aware that the author also retains the rights specified in clause 1 of the non-exclusive licence.

3. I confirm that granting the non-exclusive licence does not infringe other persons' intellectual property rights, the rights arising from the Personal Data Protection Act or rights arising from other legislation.

_____ (date)

¹ *The non-exclusive licence is not valid during the validity of access restriction indicated in the student's application for restriction on access to the graduation thesis that has been signed by the school's dean, except in case of the university's right to reproduce the thesis for preservation purposes only. If a graduation thesis is based on the joint creative activity of two or more persons and the co-author(s) has/have not granted, by the set deadline, the student defending his/her graduation thesis consent to reproduce and publish the graduation thesis in compliance with clauses 1.1 and 1.2 of the non-exclusive licence, the non-exclusive license shall not be valid for the period.*

Department of Electrical Power Engineering and Mechatronics

THESIS TASK

Student: Robin Köppe, 241398MAHM
Study programme: MAHM, Mechatronics
Supervisor(s): Mahmoud Ibrahim Hassanin Mohamed, Early Stage Researcher
Anton Rassõlkin, Tenured Associate Professor

Thesis topic:

(in English) Development of a Wheel Test Bench with its Associated Digital Twin
(in Estonian) Ratta katsestendi väljatöötamine koos sellega seotud digitaalse kaksikuga

Thesis main objectives:

1. Building the wheel test bench
2. Completing the electrical installations on the test bench
3. Create the Simulation in Simulink
4. Establish a connection between the test bench and the simulation

Thesis tasks and time schedule:

No	Task description	Deadline
1.	Building the wheel test bench	29.09.2023
2.	Completing the electrical installations on the test bench	27.10.2023
3.	Create the Simulation in Simulink	26.01.2024
4.	Establish a connection between the test bench and the simulation	29.03.2024
5.	Preparing the testing setup	26.04.2024

Language: English

Deadline for submission of thesis: "13" May 2024

Student: Robin Köppe

..... "13" May 2024
/signature/

Supervisor: Mahmoud Ibrahim Hassanin Mohamed

..... "13" May 2024
/signature/

Head of study programme: Anton Rassõlkin

..... "13" May 2024

/signature/

Terms of thesis closed defence and/or restricted access conditions to be formulated on the reverse side

CONTENTS

ABSTRACT	8
LIST OF ABBREVIATIONS AND SYMBOLS	9
1 INTRODUCTION	12
1.1 Motivation	12
1.2 Project overview	12
1.3 Thesis structure	13
2 STATE OF THE ART.....	14
2.1 Vehicle test benches	14
2.2 Digital twin technology for wheels	18
2.3 Wheel sensors	19
2.4 Chapter summary	20
3 TEST BENCH.....	21
3.1 Preparation	21
3.2 3D modelling	22
3.3 Components	23
3.3.1 Basic construction components	24
3.3.2 Mechanical components.....	25
3.3.3 Electrical components	27
3.4 Result	28
3.5 Chapter summary	29
4 SIMULATION MODEL OF THE WHEEL	31
4.1 Mathematical model of the wheel	31
4.2 Advanced mathematical model of the wheel	36
4.3 Input variables	41
5 REAL-TIME DATA EXCHANGE.....	44
5.1 Intercepting sensor data	44
5.2 Decrypting sensor data	45
5.3 Data flow to simulation	47
5.4 Simulink data implementation	48
6 TESTING	49
6.1 Setup and execution	49
6.2 Result recording.....	50
6.3 Further influencing factors.....	50
7 RESULTS AND DISCUSSION	51
7.1 Project results	51
7.2 Further developments of the test bench	52

7.3 Connection with other digital twin models	54
8 SUMMARY	56
9 KOKKUVÕTE.....	57
LIST OF FIGURES	58
LIST OF TABLES	59
LIST OF REFERENCES	60
APPENDICES	65
GRAPHICAL MATERIAL	67

ABSTRACT

The advent of autonomous vehicles marks a significant leap towards future technologies, gaining prominence in recent years. A pivotal aspect of advancing this innovation involves optimizing energy usage in self-driving electric vehicles. To this end, researchers are increasingly harnessing the synergy of real-world measurements and virtual simulations to develop digital twins (DT). Notably, the impact of the wheel components on the overall vehicle performance has been relatively underexplored. This thesis proposes the creation of a DT specifically for the vehicle's wheel. It entails the development of virtual simulation linked to empirical data collected from a custom-built test bench (TB). This TB has been designed and constructed to simulate and analyse various scenarios and factors influencing wheel dynamics under controlled laboratory conditions. Consequently, this approach will allow for a comprehensive examination of how environmental and other variables affect wheel behaviour and, by extension, the vehicle's performance.

LIST OF ABBREVIATIONS AND SYMBOLS

°	Degree (unit of angle)
°C	Degree Celsius (unit of temperature)
3D	Three dimensional
<i>a</i>	Half-length of the contact area
A	Ampere (unit of electric current)
ABS	Antilock braking system
AC	Alternating current
API	Application programming interfaces
<i>c_p</i>	Wheel stiffness
CAD	Computer-aided design
CAN	Controller area network
CEE	Commission on the Rules for the Approval of the Electrical Equipment
cm	Centimetre (unit of length)
DT	Digital twin
<i>E</i>	Modulus of elasticity
ESP	Electronic Stability Programme
EU	European Union
<i>f</i>	Deflection
<i>f_{max}</i>	Maximum deflection
<i>F</i>	Load / Force
<i>F_{max}</i>	Maximum load
<i>F_x</i>	Longitudinal force
<i>F_y</i>	Lateral force
<i>F_z</i>	Vertical wheel load
Fig.	Figure
<i>g</i>	Standard acceleration due to earth's gravity
<i>g</i>	Gramm (unit of weight)
GND	Ground
GPIO	General Purpose Input/Output
HTD	High torque drive
<i>I</i>	Area moment of inertia
IP	Internet protocol
K	Kelvin (unit of temperature)
kg	Kilogram (unit of mass)
km/h	Kilometres per hour (unit of speed)
kN	Kilonewton (unit of force)

L	Length
L	Wheel centre distance
m	Mass
m	Meter (unit of length)
m_{max}	Maximum mass
M	Torque
M_z	Self-aligning torque
MC	Microcontroller
min	Minute (unit of time)
mm	Millimetre (unit of length)
MHz	Megahertz (unit of frequency)
ms	Millisecond (unit of time)
m/s	Meters per second (unit of speed)
n	Rotational speed
n_M	Rotational speed of the motor
n_W	Rotational speed of the wheel
N	Newton (unit of force)
Nm	Newton meter (unit of torque)
P	Power
P	Wheel pressure
$P_{comparison,1}$	First reference value for the wheel pressure
$P_{comparison,2}$	Second reference value for the wheel pressure
PC	Personal computer
pt	Pneumatic trail
r	Transmission ratio / Gear ratio
r_{turn}	Vehicle turn radius
r_w	Rolling radius of the wheel
RF	Radio frequency
ROS	Robot Operation System
rpm	Rotations per minute (unit of rotational speed)
s	Second (unit of time)
SDR	Software defined radio
SMA	Sub-Miniature version A
t	Tonne (unit of mass)
t	Time
t_M	Time until reaching operating temperature
T_A	Ambient temperature
T_W	Wheel temperature

$T_{W,comparison}$	Reference value for the wheel temperature
<i>TalTech</i>	Tallinn University of Technology
<i>TB</i>	Test bench
<i>TPMS</i>	Tyre pressure monitor system
U	Circumference
<i>USB</i>	Universal Serial Bus
v	Velocity / Speed
v_{max}	Maximum speed
v_r	Linear rolling speed of the wheel
v_x	Speed in x-direction
v_y	Speed in y-direction
V	Volt (unit of voltage)
<i>VCC</i>	Voltage at collectors (positive supply voltage)
w	Width of the contact area
α	Thermal expansion coefficient
α	Lateral slip angle
β	Deviation angle of the direction of travel
γ	Wheel shaft angle
θ	Tyre stiffness
κ	Longitudinal slip
μ	Friction coefficient
σ	Theoretical slip quantity
σ_{sl}	Slip limit
Ω	Angular velocity

1. INTRODUCTION

This master's thesis is the final thesis of a master's degree in mechatronics at Tallinn University of Technology TalTech in Tallinn (Estonia) [1]. It is part of the project with the same name "Development of a test bench for wheel testing including the associated digital twin" being done by the TalTech Mechatronics and Autonomous Systems Research Group [2], [3], [4].

1.1 Motivation

It is a great opportunity for a master's student to work on a project and conduct research within a research group. In the framework of this and the preceding master's thesis in Stralsund, it was possible to gain experience in scientific work, independent research, project management and other areas. Furthermore, international participation and English as the common working language made it possible to further develop language skills.

The construction of a complex mechatronic system and the development of a DT is the perfect basis for applying the electrical engineering and mechatronic knowledge learnt during the studies. The realisation of this project challenges the skills and knowledge of an engineering graduate. This project provides the foundation for successfully completing a master's degree in mechatronics.

1.2 Project overview

The project "Development of a test bench for wheel testing including the associated digital twin" is a sub-project of the main project "Digital twin for propulsion drive of an autonomous electric vehicle" being done by the TalTech Mechatronics and Autonomous Systems Research Group [2], [5]. The overall project is funded by the Estonian Research Council under grant PSG453 [6]. It deals with the development of a DT, which combines the physical properties of the real world with a suitable virtual simulation. Applied to a propulsion drive system, the goal is to determine its most efficient use [7], [8]. As part of this project, an autonomous test vehicle called ISEAUTO was produced in 2018 and put into operation on the TalTech campus [7], [9].

During the analysis of the propulsion drive system using a DT, the influence of the wheels on the vehicle was not often considered. The aim of the project addressed in this thesis, is to consider that aspect. A TB is to be developed on which the real influences on wheels can be simulated and modified under laboratory conditions in order to investigate the behaviour of the wheels for a wide range of scenarios. Furthermore, a virtual simulation is to be created that is fed with data measured by sensors on the TB and thereby create a DT for wheels. The research group and the university provide the necessary laboratories, materials, tools, help and any other resources needed.

1.3 Thesis structure

This master thesis is divided into chapters, each of which depicts and explains a certain part of the project. The main chapters describe the state of the art, the construction of the TB, the virtual simulation of the wheel, the connection (of the TB and the simulation), the final testing and at the end a discussion of the results with an outlook on the future of the project and the further use of the TB. These chapters are each divided into sub-chapters that deal with different aspects of the topic.

2 STATE OF THE ART

The current state of the scientific knowledge in the subject area covered by the project and this thesis is summarised in this chapter. It is divided into three sub-chapters which deal with the research on TBs for electrical vehicles, DT technologies and tyre pressure monitor systems used in this context and one sub-chapter which serves as a summary of the previous ones. Therefore, multiple scientific studies and papers that deal with similar topics to the entire project or individual components of it are presented. In particular, attention is paid to other vehicle TBs, the current state of research with DTs for vehicles and the use of sensors such as tyre pressure monitor systems (TPMS) in this context.

2.1 Vehicle test benches

To improve vehicle safety, the testing of the vehicles and their components is essential to know their operational limits. In this context, various TBs were developed and used in vehicle research. Researchers usually focus on individual aspects or components of the vehicle and attempt to test their limits or behaviour in various scenarios. [10], [11], [12], [13], [14], [15]

A TB dedicated to simulating the interactions between a vehicle tyre and the road during braking conditions was proposed in [10]. It analysed the braking performance for the mixed braking system consisting of a hydraulic and an electric component. As only one wheel was set in rotation with an electric motor, it was considered that this is a simulation of a quarter of the whole vehicle. The rotating wheel was pressed with a vertical force onto an aluminium drum, which also rotated and simulated the underground. Another rotating mass was connected to this drum, which simulated the inertia of the vehicle. This TB was equipped with sensors that were all connected and communicated with the actuators. This communication took place via a vehicle control unit, in which all the data from the TB converge. It was also connected to an electronic stability programme (ESP) unit, which generated and provided the required brake pressure for the TB. In Fig. 2.1 the structure of this TB is shown. [10]

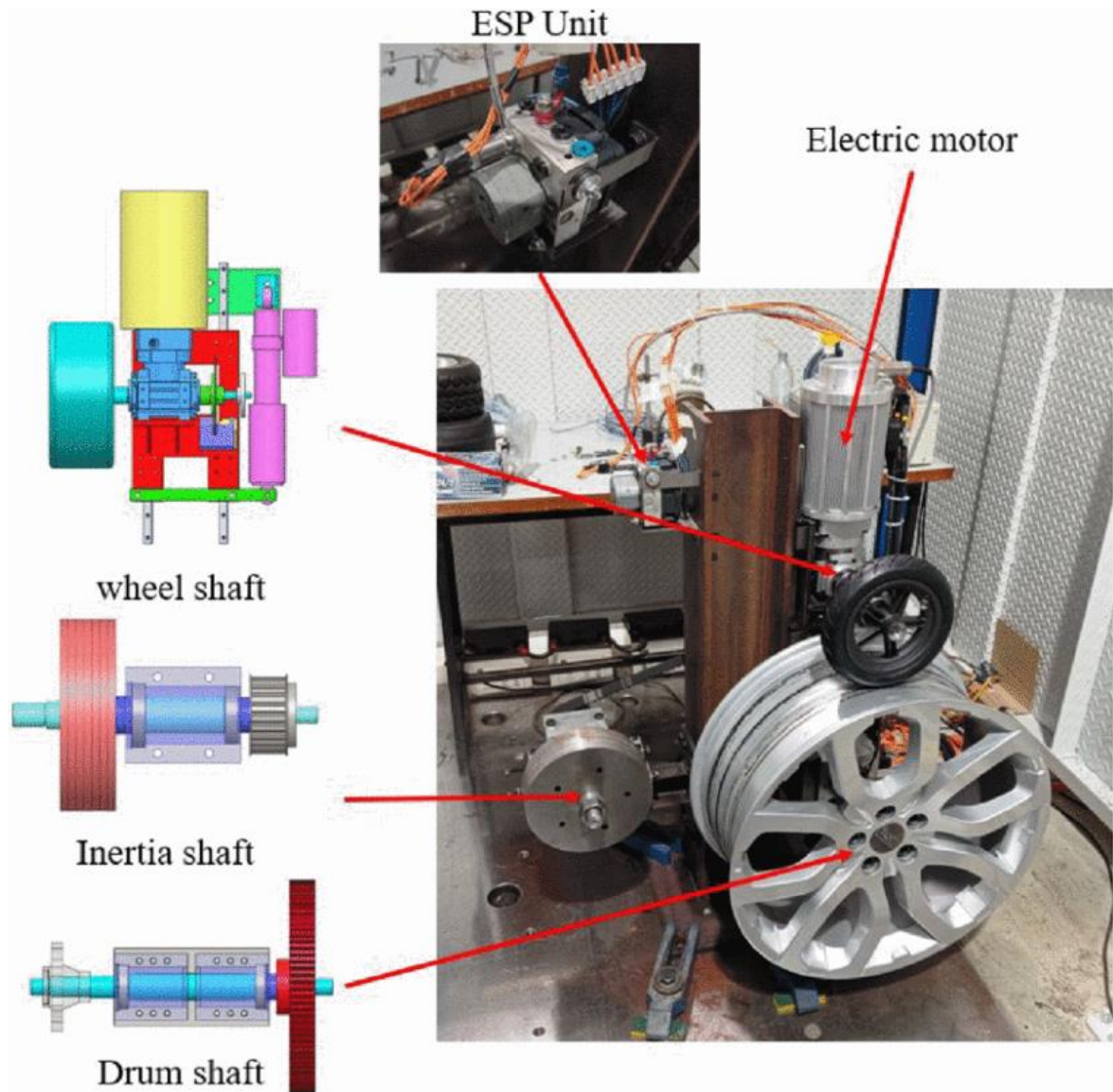


Fig. 2.1: TB for tyre-road interaction during braking [10]

Focussing on the braking process is an important aspect in this field. The research on another TB that had a similar structure and was used to investigate antilock braking systems (ABS) was discussed in [11]. In contrast to the previous TB, the ABS installed here was a completely electric ABS without hydraulic components. On this TB, on which also only one wheel was tested, a wheel-drum contact area simulated the real wheel-road contact area. This TB was able to simulate a vertical load of up to 300 kg and a speed of up to 100 km/h. Fig. 2.2 below shows a schematic overview of the TB described. [11]

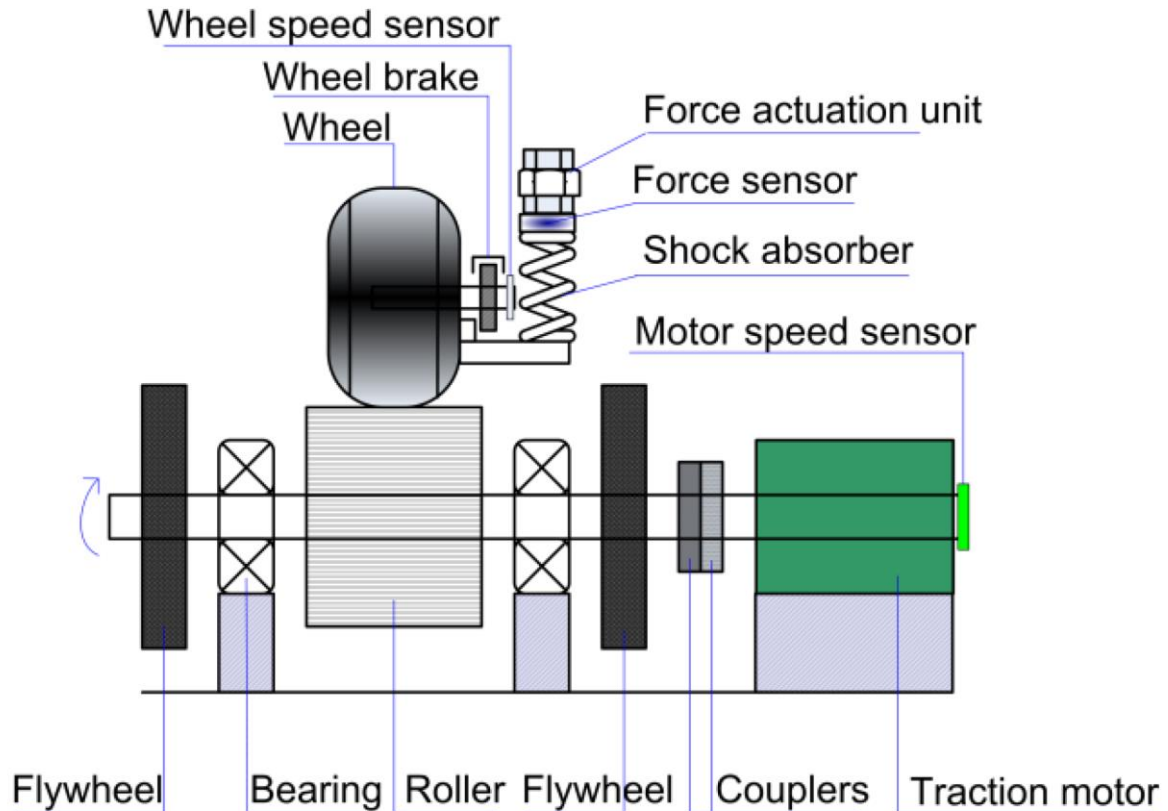


Fig. 2.2: TB diagram for all-electric ABS [11]

A single-axis closed-loop TB for improving speed measurements of wheels was proposed by J. Kres et al. in [12]. It used two redundant magneto-resistive sensors and an encoder disc, which could be arranged as required depending on the application. The TB was specially designed for determining the speed of scooters with an engine displacement of 50 cm³. The special feature of this TB was that a mathematical model was created as a counterpart, which calculated the speed of the scooter based on given input values. This model was used to create a simulation model which ran in parallel with the TB. In the simulation, influencing factors of the speed, such as the wheel circumference, could be easily adjusted. [12]

A TB made for designing a complete hybrid driving system has been discussed in [13]. It had an integrated debugging function for this hybrid driving system and was able to perform the tests automatically. Furthermore, it was designed to simulate the road load and electric load on the system using mainly an electrical power measuring system and calculate driving parameters such as the sideslip angle or longitudinal speed in real-time. The controller area network (CAN) bus technology was used for communication between the various control units, particularly due to its reliability and timeliness. [13]

Investigations of the powertrain of vehicles which also includes parameters obtained by the wheels (such as wheel radius and wheel torque) were presented by M. Gerard in [14] and P. M. Fonte et al. in [15]. A TB was created in [14] to compare different electrical vehicle powertrains by including the respective real motors and inverters, batteries and electrical control units. [14]

A TB consisting of a more detailed imitation of the powertrain of a vehicle was proposed in [15]. Two identical induction motors and the corresponding inverters were connected to each other at the motor shafts. The first motor represented the powertrain to be tested, while the second motor simulated the vehicle behaviour and the forces acting on it. CAN bus technology was also used here as a communication protocol. With this setup, various dynamic tests were able to be carried out for different vehicles, as different motors, wheels, batteries, gears or cooling systems can be chosen. A schematic overview of the overall TB setup is shown in Fig. 2.3. [15]

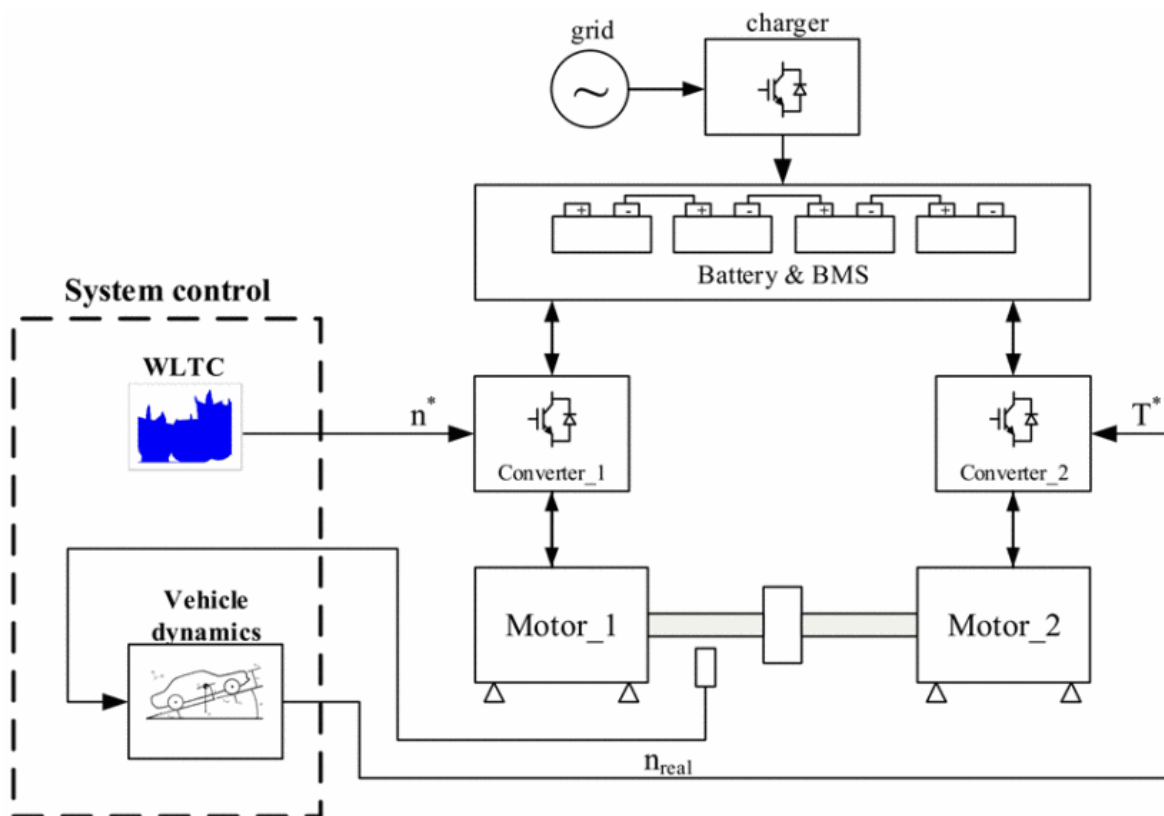


Fig. 2.3: Illustrative diagram of a powertrain TB [15]

2.2 Digital twin technology for wheels

DTs have become more common in research on autonomous vehicles in recent years. These DTs combine measurement data from reality with simulations in real-time and thus generate a digital copy of this reality. This makes it possible to obtain feedback in real-time or even predict the behaviour of the vehicle for various scenarios (which are reflected by various simulations). Studies that have dealt with this topic have proposed the optimisation of the electric drive of vehicles with the help of DTs. A requirement for this is the development of physical models of the various components of the vehicle's drive system. The corresponding models are then to be created (in the programme MATLAB for example) to be able to develop a DT of the entire system in the end. The data for the models are often provided using the Linux Robot Operation System (ROS) like in [16]. The main components of the DT are the real physical object, the virtual model, the service system, the DT data and the connection of all of these components. The interaction of all these components is illustrated in Fig. 2.4. [7]

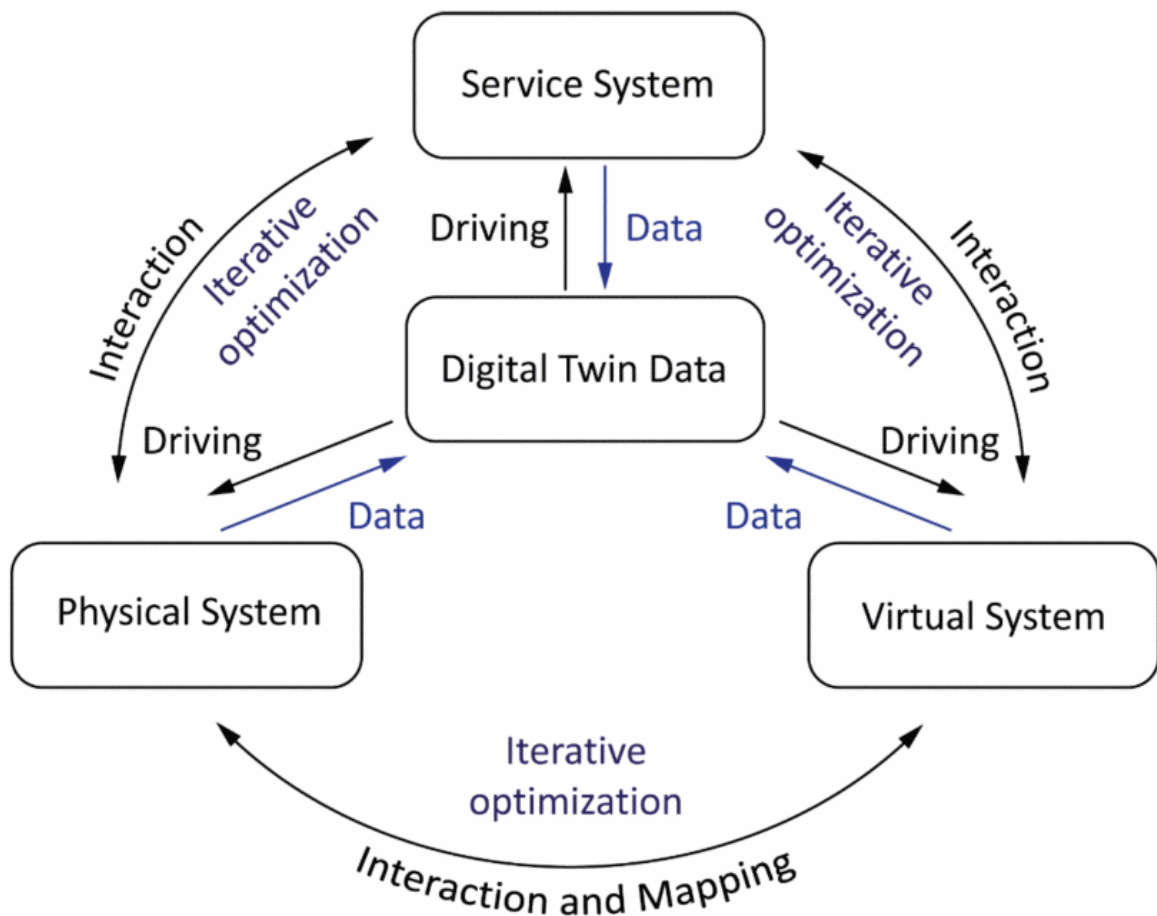


Fig. 2.4: Structure of a DT [7]

In a study carried out by M. S. Elbakry et al. in [17], a methodology for the creation of a DT simulation architecture for connected and automated vehicles was proposed, which consisted of two main layers. One replicated the physical environment and the other the digital environment. Voltage and speed sensors were used to collect vehicle data such as the wheel speed. [17]

A DT dealing with wheels of vehicles was proposed by S. Venturini et al. in [18]. However, this DT focused on the prediction of material failure of the steel rims of the wheels during material fatigue tests. A TB was also developed, which can be used to test different load influences, among other things. Wheel pressure was also taken into account for the calculations of the simulation. In this case, virtual sensors were primarily used as sensors for the changes in the rim like cracks. [18]

2.3 Wheel sensors

The volume of traffic has steadily increased over the past years and decades. TPMS are used to guarantee the safety of motor vehicles by constantly checking the tyre pressure of the vehicles. The first TPMS were installed in the USA in 1907 [19]. Such systems were then implemented in vehicles in Europe for the first time in 1986 with the "Porsche 959" [20]. TPMS are installed in a vehicle and use sensors in or on the tyre to monitor the tyre pressure and its change over time. This information is transmitted to the driver in real-time. Regulation No. 661/2009 of the European parliament and of the council stipulates that since November 2012, all new vehicles registered in the EU with a mass of up to 3500 kg must have a TPMS installed [21].

There are two main types of TPMS sensors that can be used to collect and transmit data [22]. On the one hand, external sensors can be used, which are screwed onto the outside of the tyre valve and are therefore easy to install. On the other hand, built-in sensors can be used, which are attached to the rim in the inside of the tyre. These have a longer battery life and are more accurate but are more complicated to fit and replace. Both types of sensors measure the tyre pressure and optionally the wheel temperature and send these data at a radio frequency (of usually 433 MHz in Europe) to a receiver module. This module is connected to a monitor that displays the data to the driver. How precisely these measurements work was tested and discussed by S. Gryś in [19] using a TB. It concluded that in order to obtain accurate measurement results, a calibrated sensor should be used, which in the best case has been calibrated using the methodology of least squares multi-point fitting. [19]

An identification scheme for the friction coefficient between the wheel and the road was proposed by R. Matsuzaki et al. in [23]. Influencing factors such as the slip angle or the lateral force acting on the wheel were also taken into account. A three-axis accelerometer was used as a sensor to measure the deformation of the tyre during cornering. [23]

Another way of measuring the wheel-road friction coefficient was discussed by F. Holzmann et al. in [24]. In this study, a camera and a microphone were used as sensors together with an algorithm developed for this purpose. After several test series with this method, the friction coefficient was divided into six different classes in addition to the stop range of 0 to 0,15. These were icy surface (0,15 – 0,3), wet surface (0,3 – 0,45), humid cobblestone (0,45 – 0,55), bad coefficient (0,55 – 0,65), middle coefficient (0,65 – 0,7) and excellent coefficient (0,7 – 1). It was also noted that these correlations may vary slightly depending on the tyre and vehicle. [24]

2.4 Chapter summary

Based on the literature review presented above, the following correlation between the individual sub-chapters can be established. In the research field of electric vehicles there are already many TBs for investigating the wheel dynamics and behaviour of the vehicle in different situations. Most of them relate to specific areas like the braking process of the wheels, the material fatigue of the steel rim, or the entire power train of the vehicle. Research on DTs in relation to electric vehicles has made great progress in recent years, but often the influence of the wheels on the driving behaviour has not been considered separately. The use of TMPS sensors in this context is reliable under certain conditions, as further research has shown. Predictive methods for other influencing factors such as the friction coefficient are possible but more complicated to implement.

Considering the information mentioned above, the idea of developing a TB specialised on analysing the wheel behaviour separately together with the associated DT was created. This TB must be able to imitate various states of the wheel (standstill, acceleration, braking, etc.) and be directly connected to the virtual simulation created for this purpose.

3 TEST BENCH

This chapter deals with the construction of the TB. The aim of the TB is to emulate the wheel's rotation as realistic as possible under laboratory conditions. The sensors attached to the wheel collect data in real-time and send it to the simulation model in order to create a DT of the wheel.

Before the construction, preparation is needed. Therefore, a 3D model of the TB was developed. The individual components were then selected, ordered and assembled. Finally, the sensors and electrical components were installed. These individual steps are explained in the following and then discussed in the end. A more detailed description of the construction can be found in the other master's thesis that preceded this one [4].

3.1 Preparation

Good preparation is necessary to carry out a successful construction. Firstly, the requirements that TB must fulfil are discussed and defined. These result mainly from the goal of imitating the movement and behaviour of wheels during driving as realistically as possible under laboratory conditions.

The influencing factors should first be defined and later tried to be simulated with the TB. These are not static, but changing, which is why they should also be adjustable on the TB (if possible). This allows to simulate and test different scenarios. In the reality, a wide range of factors influence the behaviour of the wheels. The following ones are defined as the main influencing factors that should be attempted to be simulated (adjustable) on the TB.

- Wheel pressure
- Wheel temperature
- Angle of the wheel
- Environmental temperature
- Weight of the vehicle
- Friction between the wheel and the surface
- Load (less load if vehicle goes downhill, more load if vehicle goes uphill)

Based on the above, the following capabilities and requirements are defined, which the TB should fulfil. A detailed description of the individual points can be found in the preceded master's thesis [4].

- Ability to fit a car wheel
- Underground mounting capability
- Wheel rotation
- Adjustable wheel pressure
- Adjustable wheel angle
- Adjustable wheel load (on the underground)
- Speed adjustability
- Emergency stop implementation
- Stability
- Safety
- Cost efficiency
- Limited space

3.2 3D modelling

One of the most important steps before the TB construction begins is the creation of a 3D model, which serves as a template. The rough ideas are first recorded with pen and paper and later finalised in the 3D model. The model makes it possible to recognise and solve problems before the construction starts. This applies to the arrangement, size and shape of the individual components. Furthermore, it is much easier to discuss important decisions in the team with a model as visual support.

The 3D model is created using the 3D CAD programme "SOLIDWORKS" from "Systèmes SolidWorks Corporation" [25]. By using the software, it is possible to create all the components individually and combine them into a merged model by defining mutual relations. This allows errors to be recognised at an early stage and the individual components to be continuously edited or moved if discrepancies occur. In this way, a model of the TB is gradually created, which serves as a template for selecting and ordering the individual components and for the actual construction.

The final 3D model is shown in Fig. 3.1. It contains all the important dimensions for the structure of the TB. Details such as the teeth of the gears or smaller components such as screws and the floor protection are negligible for the space planning and are therefore not shown in the model. For some components such as the aluminium profiles or the bearings of the wheel shaft, 3D templates are provided by the manufacturers [26], [27], [28]. Another important point is the insertion of placeholders for future components, such as the underground. For this purpose, a treadmill on which the wheel runs will be inserted into the TB in later steps.

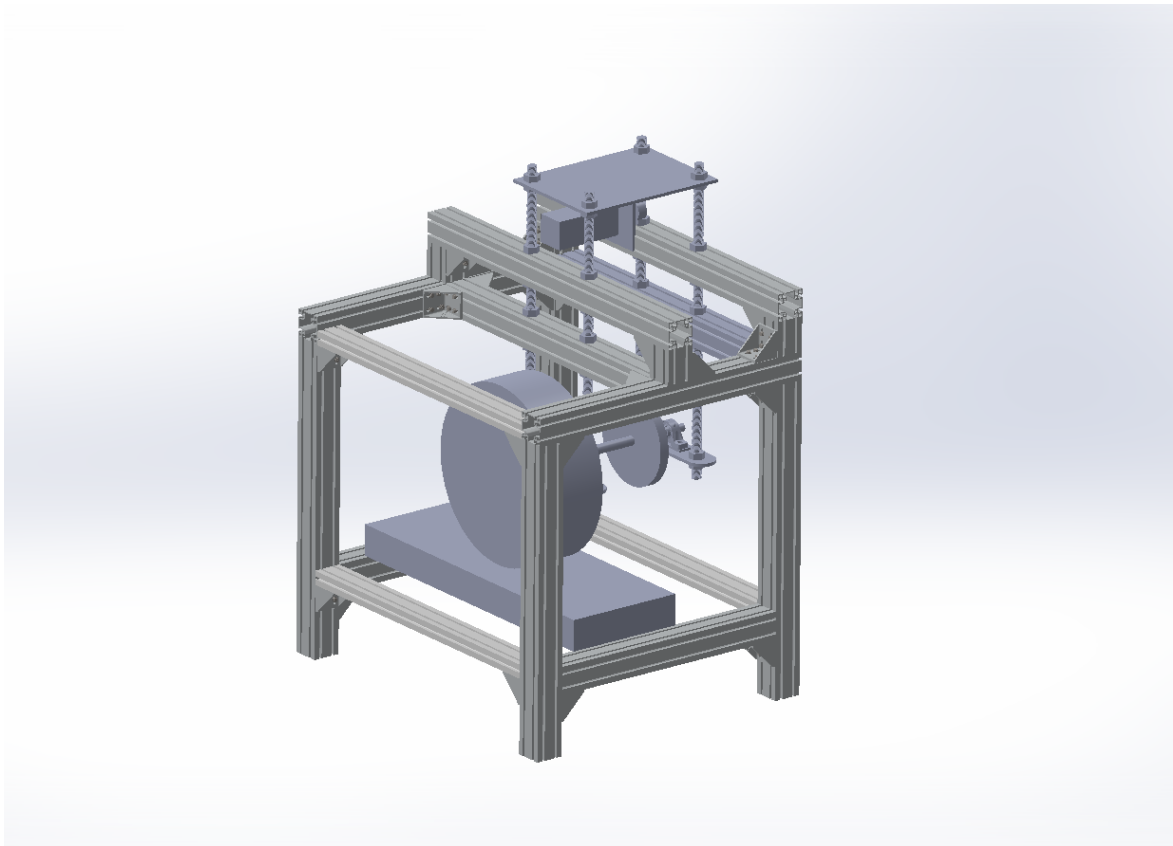


Fig. 3.1: TB 3D model

The model fulfils the requirements. It provides an overview of which components need to be ordered for the TB and how they are arranged and connected to each other. It is not suitable for providing detailed information, such as the number of screws required. Despite conscientious planning, it must be assumed that individual components cannot be delivered on time or have dimensions that deviate from the description. Therefore, these must be continuously checked and, if necessary, adjusted in the model. It is assumed that the construction of the TB can be carried out successfully and efficiently using the model.

3.3 Components

Various components and parts are required for the construction of the TB, which are briefly described below. A distinction is made between basic construction components, mechanical components and electrical components. The tools used for the construction are not mentioned here.

3.3.1 Basic construction components

The basic construction of the TB consists of an aluminium profile system from "MiniTec". 90x90 mm and 45x90 mm profiles are used for the construction of the TB [29]. They are made of the aluminium alloy EN-AW-6063 T66 with the material number 3.3206.72 and a specific weight of 2,75 g/cm³ [29]. The profiles are connected with matching aluminium angles and eight screws per angle [30]. Two holes are drilled in four of the profiles for a total of four threaded rods which transfer the main load into the profiles [31]. This load consists mainly of three steel plates to which the motor and, via two bearings, the wheel shaft and wheel are attached [32]. The contact surfaces of the profiles with the floor are covered with 3D printed caps to protect the laboratory floor.

The choice of profiles is made based on load capacity calculations. For stability and safety reasons the aluminium profiles should not bend more than 0,5 mm under load. The four profiles that carry the main load are each 1,00 m long. The mass of the main functional unit of the TB corresponds to approximately 100 kg (threaded rods, motor, steel plates, bearings, wheel, wheel shaft, etc.), which corresponds to approximately 25 kg per profile. As these profiles also must absorb a lot of kinetic energy during operation of the TB and as they are likely to lose some of their stability due to the drilled holes, a tolerance of 1000% is applied, which corresponds to a maximum mass m_{max} of 250 kg on each profile. Considering the standard acceleration due to earth's gravity g of 9,81 m/s², this corresponds to the following maximum load F_{max} per profile calculated in equation (3.1)

$$F_{max} = m_{max} * g = 250 \text{ kg} * 9,81 \frac{\text{m}}{\text{s}^2} = 2452,5 \text{ N}, \quad (3.1)$$

where F_{max} – maximum load, N,

m_{max} – maximum mass, kg,

g – standard acceleration due to earth's gravity, m/s².

Furthermore, the manufacturer provides the following equation (3.2) which is used to calculate the deflection for profiles that are supported on both sides only at the bottom as on the TB [29]. The basis for the calculation is the required maximum deflection f_{max} of 0,5 mm, the free length L of 1,00 m of each profile and the modulus of elasticity of aluminium E of 70000 N/mm². The area moment of inertia I is calculated in equation (3.3), which can be used to find the appropriate aluminium profile in a table provided with the equation

$$f = \frac{F * L^3}{E * I * 48 * 10^4}, \quad (3.2)$$

where f – deflection, m,

F – load, N,

L – free length, m,

E – modulus of elasticity, N/mm²,

I – area moment of inertia, kg*m²,

$$I = \frac{F_{max} * L^3}{E * 48 * 10^4 * f_{max}} = \frac{2500 \text{ N} * (1000 \text{ mm})^3}{70000 \frac{\text{N}}{\text{mm}^2} * 48 * 10^4 * 0,5 \text{ mm}} = 148,81 \text{ kg} * \text{m}^2, \quad (3.3)$$

where f_{max} – maximum deflection, m.

With an area moment of inertia I of 230 kg*m², the 90x90 mm aluminium profile is the only one that bends less than 0,5 mm at the maximum load and therefore fulfils the stability and safety requirements [29]. For non-loaded connections, 45x90 mm profiles (vertical: 110 kg*m², horizontal: 27 kg*m²) are used.

3.3.2 Mechanical components

The motor used on the TB is a 3-phase induction motor from "ABB" of the type QY80M2A. This motor has a rated rotational speed of 2840 rpm at a rated frequency of 50 Hz, a rated power of 0,75 kW, a rated current of 2,95 A and a rated voltage of 220-240 V for the delta configuration which is used in this case. The shaft has a diameter of 19 mm. The motor is mounted upside down with screws to the top steel plate.

A gear is attached to the shaft of the motor using a suitable taper-lock bush [33], [34]. The taper-lock bush is of the type 1108 19, has an internal diameter of 19 mm and a slightly conical shape on the outside [35]. It is placed on the shaft and tightened with the corresponding screws. A suitable gear is attached on the outside with two screws. The smallest gear of the type 8M (8 mm distance between the individual teeth) and high torque drive (HTD) with 24 teeth is selected for this [36]. A matching 20 mm wide and 1,76 m long tooth belt, also of type HTD 8M, is used [37]. It serves as a rotational movement transmitter between the motor shaft and wheel shaft and is tensioned by screwing the steel plates down or up on the threaded rods. For the gear of the wheel shaft, the largest available of the type HTD 8M one with 112 teeth is selected [38]. It

can be firmly connected to the wheel shaft with a 27 mm drilled inner hole and a welded-on metal piece with three tightening screws, each offset by 120° and vertical to the shaft.

This wheel shaft is approximately 55 cm long and connected at the end to a car wheel of the type 175/70 R 13 82H from "Michelin". The wheel shaft is slightly conical and is ground down with a high degree of precision to a diameter of 30 mm, 27 mm and 25 mm at three suitable sections. This design ensures that the wheel shaft and wheel can be easily dismantled if necessary and reassembled later. The 27 mm section is intended for the gear and the 30 mm and 25 mm diameter sections for the two bearings in which the wheel shaft rotates. Bearings of the type UCP 205/H and UCP 206/H from "SKF" are used [27], [28]. These fulfil the requirements with limiting speeds of 5850 rpm and 5000 rpm, supported dynamic loads of up to 14 kN and 19,5 kN and supported static loads of up to 7,8 kN and 11,2 kN [27], [28]. Furthermore, the bearings withstand alternating rotations and therefore also function when the wheel shaft is brought into a slight angle to them. They are mounted on the lower steel plates.

The different size of the gears is chosen to obtain a transmission ratio, as the motor can rotate faster than required, but as much power as possible should be utilised. Due to the in equation (3.4) shown inversely proportional relationship between the torque M and the rotational speed n at constant power P , the rotational speed can be reduced and the torque at the wheel can be increased with a transmission ratio according to

$$P = 2 * \pi * M * n, \quad (3.4)$$

where P – power, W,

M – torque, Nm,

n – rotational speed, s⁻¹.

The value of the transmission ratio r is calculated in equation (3.5)

$$r = \frac{112}{24} = 4,67, \quad (3.5)$$

where r – transmission ratio.

This transmission ratio of 4,67 means that the in equation (3.9) calculated maximum speed of the wheel v_{max} can be generated at the maximum rotational speed of the motor n_M of 2840 rpm. This is calculated considering the measured wheel circumference U of

1,79 m and by calculating the rotational speed of the wheel n_W in the equation (3.6), (3.7) and (3.8)

$$n_M = 2840 \text{ rpm} = 47,33 \text{ s}^{-1}, \quad (3.6)$$

where n_M – rotational speed of the motor, s^{-1} ,

$$r = 4,67 = \frac{n_M}{n_W}, \quad (3.7)$$

where n_W – rotational speed of the wheel, s^{-1} ,

$$n_W = \frac{n_M}{r} = \frac{47,33 \text{ s}^{-1}}{4,67} = 10,14 \text{ s}^{-1}, \quad (3.8)$$

$$v_{max} = n_W * U = 10,14 \text{ s}^{-1} * 1,79 \text{ m} = 18,14 \text{ m/s} = 65,31 \text{ km/h}, \quad (3.9)$$

where U – circumference, m,

v_{max} – maximum speed of the wheel, m/s.

This maximum speed of 65,31 km/h is sufficient. As a minibus designed for the university campus, ISEAUTO is allowed to travel at a maximum speed of 20 km/h [7]. At this wheel speed on the TB, the motor is utilised to 30,6 %. In order to be able to test the wheels for extreme situations, the TB should be able to bring wheels to speeds of up to 50 km/h, which is also possible.

3.3.3 Electrical components

Electrical components are also required to operate the TB and carry out tests with it. These components are mainly responsible for controlling the motor and collecting data. The most important sensor is positioned on the wheel cap valve to measure the tyre pressure and temperature. A TPMS from "Jansite" is used for this purpose [22]. The sensor continuously transmits the data to a small monitor via a radio signal. A microcontroller (MC) from "Raspberry Pi" is used together with a suitable 433 MHz radio frequency module receiver to intercept these signals and forward them to the simulation model [39], [40].

A frequency converter of the type ACS850-04-018A-4 from "ABB" is used to control the motor. It has an input range of 380-480 V AC at 48-63 Hz and is operated via a 400 V CEE socket at 50 Hz at the TB. The output is a variable frequency from 0 to 500 Hz which is sufficient to operate the motor. The motor can be controlled via a connected keypad from ABB. In addition, an on/off switch has been installed which can be used to switch the frequency converter on and off. The frequency converter is attached to an aluminium profile at the right side of the TB.

3.4 Result

The TB was successfully developed and positioned in the laboratory setup. It is 1,18 m wide, 0,98 m long and 1,58 m high and has an approximate weight of 500 kg. It can be started by connecting it to a 400 V CEE socket and switching on the frequency converter under the keypad. The whole TB is grounded for a safe operation. The current status of the TB is shown in Fig. 3.2. It should only be operated or further modified by instructed persons.



Fig. 3.2: Wheel TB

3.5 Chapter summary

The TB meets the requirements and works as planned. A car wheel like the one used on the ISEAUTO is installed and can be brought into a controllable rotational movement using the motor. Via the frequency converter keypad this movement can be started and stopped, and the speed can be adjusted. The valve of the wheel is still accessible, which also allows the wheel pressure to be changed. The angle at which the wheel rotates in relation to the underground can be adjusted by changing the height of just one of the two steel plates on which a bearing is mounted. Thanks to the use of strong aluminium profiles, the TB is stable and safe and can also withstand heavy loads during operation.

The risks while using the TB have been minimised. In addition to the easy accessible on/off switch an aluminium profile was installed at the top front of the TB which serves as a barrier in front of the rotating wheel. Furthermore, the TB was completely grounded. The TB also successfully fits inside of the available space and is within the budget.

No underground has been installed on the TB so far, which means that the wheel initially rotates in the air and no different vehicle weights are simulated by pressing the wheel onto the underground. The procurement and installation of a suitable underground is complex and not necessary for the development of the DT within the framework of this thesis. However, some preparations such as the installation of 90 x 90 mm aluminium profiles that can withstand maximum loads at the corresponding places in the lower area of the TB have already been made. Corresponding calculations have also already been carried out and are explained in more detail in the outlook in chapter 7.2.

4 SIMULATION MODEL OF THE WHEEL

This chapter deals with the simulation of wheels. The aim of the simulation is to create a digital copy of the wheel behaviour in the reality. The programme used for the simulation is "MATLAB" in version "R2023b" and the associated add-on product "Simulink" from "The MathWorks, Inc." [41]. The aim is to feed this simulation with the data of the influencing factors that also affect the wheel in reality and by that generate a DT. The simulation should replicate the behaviour of the wheel as closely as possible using suitable calculations and correlations.

4.1 Mathematical model of the wheel

As part of the project, a simulation for wheels was developed in advance, which serves as the starting point for this thesis [42]. It was further developed for being used together with the TB and adapted to the requirements of the DT. This chapter provides an overview of how the simulation has worked so far and the next one explains the changes that have been made.

The starting point for the calculations is the definition of the lateral slip angle α and longitudinal slip κ . These change as follows depending on the driving behaviour of the vehicle [42]. When the vehicle is driving and the wheels are therefore rotating in the same speed as the vehicle is moving, the longitudinal slip κ has the value shown in equation (4.1)

$$\kappa = 0, \tag{4.1}$$

where κ – longitudinal slip.

If the vehicle brakes and the wheels do not turn or turn slower than the vehicle is moving, the longitudinal slip κ has the value shown in equation (4.2)

$$-1 \leq \kappa < 0. \tag{4.2}$$

If the vehicle is accelerating and the wheels are turning faster than the vehicle is moving, the longitudinal slip κ has the value shown in equation (4.3)

$$0 < \kappa \leq 1. \quad (4.3)$$

If the vehicle is travelling straight ahead and no lateral forces are acting on it, the lateral slip angle α has the value shown in equation (4.4)

$$\alpha = 0. \quad (4.4)$$

where κ – slip angle, °.

If the direction of travel of the vehicle deviates from its geometric alignment and it oversteers inwards, the lateral slip angle α has the value shown in equation (4.5)

$$0 < \alpha \leq 90^\circ = \frac{\pi}{2}. \quad (4.5)$$

If the direction of travel of the vehicle deviates from its geometric alignment and it oversteers outwards, the lateral slip angle α has the value shown in equation (4.6)

$$-90^\circ = -\frac{\pi}{2} \leq \alpha < 0. \quad (4.6)$$

Next, the theoretical slip quantity σ is defined in equation (4.9) (as vector $\vec{\sigma}$) and (4.10) (as vector length σ). This indicates how much the wheel slips in comparison to the speed. It consists of the theoretical slip quantity in the x-direction σ_x calculated in equation (4.7) and the theoretical slip quantity in the y-direction σ_y calculated in equation (4.8)

$$\sigma_x = \frac{\kappa}{\kappa + 1}, \quad (4.7)$$

where σ_x – theoretical slip quantity in the x-direction,

$$\sigma_y = \frac{\tan(\alpha)}{\kappa + 1}, \quad (4.8)$$

where σ_y – theoretical slip quantity in the y-direction,

$$\vec{\sigma} = \begin{pmatrix} \sigma_x \\ \sigma_y \end{pmatrix}, \quad (4.9)$$

where σ – theoretical slip quantity,

$$\sigma = \sqrt{\sigma_x^2 + \sigma_y^2}. \quad (4.10)$$

After that the half-length of the contact area a is calculated. It is assumed that this contact area is a rectangle, which can be defined by multiplying the length of the contact area $2a$ and the width of the contact area w [42]. While the width of the contact area w is given, the half-length of the contact area a is calculated in equation (4.11), taking into account the given wheel pressure P and the given vertical wheel load F_z

$$a = \frac{F_z}{2 * P * w}, \quad (4.11)$$

where a – half-length of the contact area, m,

F_z – vertical wheel load, N,

P – wheel pressure, bar,

w – width of the contact area, m.

Based on this, the tyre stiffness θ is now calculated in equation (4.12). In addition to the half-length of the contact area a , the given values for the wheel stiffness c_p , the friction coefficient μ and again the vertical wheel load F_z are required for this

$$\theta = \frac{2 * c_p * a^2}{3 * \mu * F_z}, \quad (4.12)$$

where θ – tyre stiffness,

c_p – wheel stiffness, N/m²,

μ – friction coefficient.

The reciprocal of the tyre stiffness θ is the slip limit σ_{Sl} , from which the wheel starts to slide over the surface. It is calculated in equation (4.13)

$$\sigma_{sl} = \frac{1}{\theta}, \quad (4.13)$$

where σ_{sl} – slip limit.

From this point on, a distinction is made whether this slip limit σ_{sl} is exceeded or not. In other words, whether the wheel slips over the surface (full slip) or not (partial slip). Finally, the three outputs of the simulation are calculated. These are the longitudinal force F_x , the lateral force F_y and the self-aligning torque M_z . The two forces are calculated in the equations (4.16) and (4.17) with the help of the combined force F as vector \vec{F} in equation (4.14) and as vector length F in equation (4.15)

$$\vec{F} = \begin{pmatrix} F_x \\ F_y \end{pmatrix} = F * \frac{\vec{\sigma}}{\sigma}, \quad (4.14)$$

where F – combined force, N,

F_x – longitudinal force, N,

F_y – lateral force, N,

$$F = \sqrt{F_x^2 + F_y^2} = \begin{cases} \mu * F_z * [3 * \theta * \sigma - 3 * (\theta * \sigma)^2 - (\theta * \sigma)^3] & \text{for } \sigma \leq \sigma_{sl} \\ \mu * F_z & \text{for } \sigma > \sigma_{sl} \end{cases}, \quad (4.15)$$

$$F_x = F * \frac{\sigma_x}{\sigma} = \begin{cases} \frac{\sigma_x}{\sigma} * \mu * F_z * [3 * \theta * \sigma - 3 * (\theta * \sigma)^2 - (\theta * \sigma)^3] & \text{for } \sigma \leq \sigma_{sl} \\ \frac{\sigma_x}{\sigma} * \mu * F_z & \text{for } \sigma > \sigma_{sl} \end{cases}, \quad (4.16)$$

$$F_y = F * \frac{\sigma_y}{\sigma} = \begin{cases} \frac{\sigma_y}{\sigma} * \mu * F_z * [3 * \theta * \sigma - 3 * (\theta * \sigma)^2 - (\theta * \sigma)^3] & \text{for } \sigma \leq \sigma_{sl} \\ \frac{\sigma_y}{\sigma} * \mu * F_z & \text{for } \sigma > \sigma_{sl} \end{cases}. \quad (4.17)$$

The last step is the calculation of the self-aligning torque M_z in equation (4.19). For this purpose, the pneumatic trail ρt is calculated in equation (4.18) as an intermediate variable, which is a measure to indicate how far the wheel contact area is behind the centre of gravity line of the vehicle. The self-aligning torque M_z is then calculated with the help of this factor and the lateral force F_y acting on the wheel

$$pt = \begin{cases} \frac{a}{3} * \frac{1 - 3 * \theta * \sigma - 3 * (\theta * \sigma)^2 - (\theta * \sigma)^3}{1 - \theta * \sigma + \frac{1}{3} * (\theta * \sigma)^2} & \text{for } \sigma \leq \sigma_{Sl} \\ 0 & \text{for } \sigma > \sigma_{Sl} \end{cases}, \quad (4.18)$$

where pt – pneumatic trail, m,

$$M_z = pt * F_y, \quad (4.19)$$

where M_z – self-aligning torque, Nm.

To summarise, this model can be used to calculate the longitudinal force F_x , the lateral force F_y and the self-aligning torque M_z from the lateral slip angle α , the longitudinal slip κ , the width of the contact area w , the wheel pressure P , the vertical wheel load F_z , the wheel stiffness c_p and the friction coefficient μ . The rolling resistance is neglected and it is assumed that the wheel stiffness c_p and the friction coefficient μ are constant and that the pressure is distributed parabolic over a rectangular contact area [42].

The Simulink model, which simulates the behaviour of the wheel, consists of several function blocks. These reflect the logic of the mathematical relationships listed above. An overview of the model is shown in Fig. 4.1.

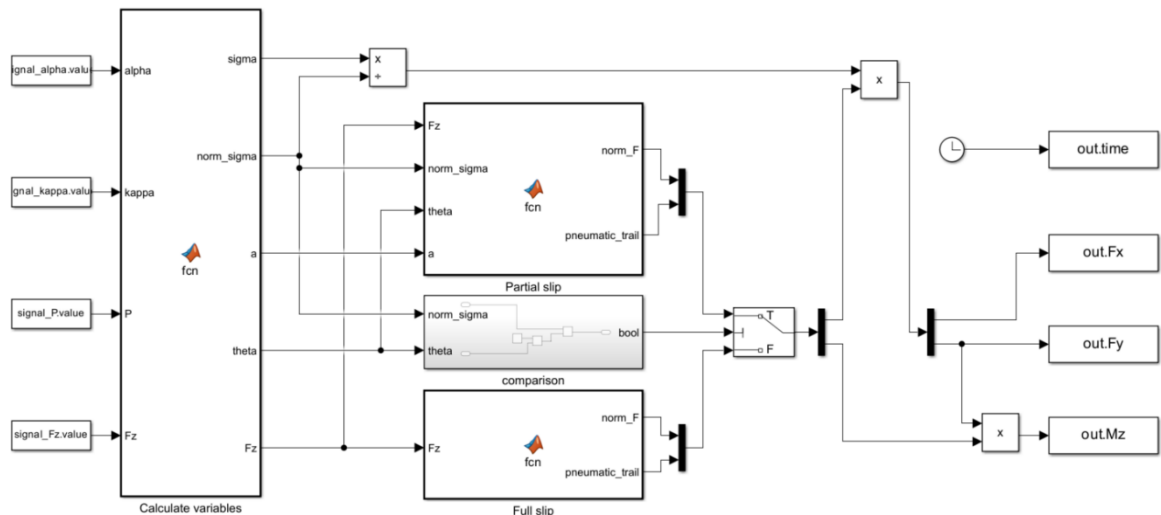


Fig. 4.1: Simulink model [42]

In the first function block "Calculate variables", the values for the half-length of the contact area a , the tyre stiffness θ and the theoretical slip quantity σ (as vector $\vec{\sigma}$ and as vector length σ) are calculated based on the formulas described above. The predefined values for the lateral slip angle α , the longitudinal slip κ , the wheel pressure P , the vertical wheel load F_z , the wheel stiffness c_p , the friction coefficient μ and the width of the contact area w serve as inputs for this.

The values for the resulting force F and the pneumatic trail pt are then calculated in the two function blocks "Partial slip" and "Full slip". In the "Partial slip" block (which is used for $\sigma \leq \sigma_{sl}$), the vertical wheel load F_z , the theoretical slip quantity σ , the tyre stiffness θ , the half-length of the contact area a and the friction coefficient μ are required. In the "Full slip" block (which is used for $\sigma > \sigma_{sl}$), only the vertical wheel load F_z and the friction coefficient μ are required to calculate the force F , as the pneumatic trail is zero at full slip.

To decide which of the two blocks should be used, there is a further "Comparison" block in which the slip limit σ_{sl} is calculated from the tyre stiffness θ and compared to see whether the current theoretical slip quantity σ exceeds it (full slip) or is below it (partial slip). Depending on the result of this comparison, the appropriate values for the resulting force F and the pneumatic trail pt are used to calculate the outputs of the simulation.

The longitudinal force F_x and the lateral force F_y from the theoretical slip quantity σ and the resulting force F as well as the self-aligning torque M_z from the lateral force F_y and the pneumatic trail pt are calculated as outputs according to the formulas. These outputs can then be plotted and visualised as a function of the slip angle α or the longitudinal slip κ , for example.

4.2 Advanced mathematical model of the wheel

This chapter explains the changes made to the previously presented model. In addition to the previously considered influencing factors wheel pressure and vertical wheel load, the main aim is to integrate the influencing factors wheel speed, wheel temperature and wheel angle, which are already measurable (and partially adjustable) on the TB, as well as the influencing factor ambient temperature, which will be measurable (and partially adjustable) on the TB in the future. The mathematical relationships based on which these integrations take place are first explained and then the changes made to the simulation are shown.

In the first step, the influence of the angle of the wheel shaft of the TB to the ground γ is to be integrated. This is normally zero, as the wheel is at a right angle to the underground and the wheel shaft drives the wheel horizontally to the underground. However, this angle changes slightly on a sloping surface or when driving a curve. It can also be changed on the TB by screwing the corresponding steel plates on which the wheel shaft bearings sit up or down. This change also results in a deviation angle of the direction of travel β calculated in equation (4.22). Equations (4.20) and (4.21) are used to form equation (4.22) [43], [44]. Therefore, the wheel speed v and wheel shaft angle γ set on the TB as well as the vehicle turn radius r_{turn} and the constant values for the wheel centre distance L (the distance between the front and rear axle of the vehicle) and the standard acceleration due to earth's gravity g are used

$$r_{turn} = \frac{L}{\sin(\beta)}, \quad (4.20)$$

where r_{turn} – vehicle turn radius, m,

L – wheel centre distance, m,

β – deviation angle of the direction of travel, °,

$$\gamma = \arctan\left(\frac{v^2}{g * r_{turn}}\right), \quad (4.21)$$

where γ – wheel shaft angle, °,

v – wheel speed, m/s,

$$\beta = \arcsin\left(\frac{L * g * \tan(\gamma)}{v^2}\right). \quad (4.22)$$

As the vehicle then has a lateral delay in the direction of travel, the speed in the x-direction v_x is calculated in equation (4.23) and in the y-direction v_y in equation (4.24) depending on the speed and the previously calculated deviation angle of the direction of travel β

$$v_x = v * \cos(\beta), \quad (4.23)$$

where v_x – speed in x-direction, m/s,

$$v_y = v * \sin(\beta), \quad (4.24)$$

where v_y – speed in y-direction, m/s.

Then the linear rolling speed of the wheel v_r is introduced. It can be described as the product of the rolling radius of the wheel r_w and the angular velocity Ω as shown in equation (4.25) [42]. The linear rolling speed v_r is zero if braking is simulated and the wheel is therefore not turning. It corresponds to the speed of the wheel in the x-direction v_x when driving is simulated and the wheel is therefore turning. This relation is shown in equation (4.26)

$$(v_r = r_w * \Omega), \quad (4.25)$$

where v_r – linear rolling speed, m/s,

r_w – rolling radius of the wheel, m,

Ω – angular velocity, s^{-1} ,

$$v_r = \begin{cases} 0 & \text{for driving} \\ v_x & \text{for braking} \end{cases} \quad (4.26)$$

The lateral slip angle α in equation (4.27) and the longitudinal slip κ in equation (4.28) can now be calculated based on these three velocities [42], [45]. These calculations therefore replace the previously changeable variables for the lateral slip angle and the longitudinal slip

$$\alpha = \arctan\left(\frac{v_y}{|v_x|}\right), \quad (4.27)$$

$$\kappa = -\frac{v_x - v_r}{v_x}. \quad (4.28)$$

In the next step, the influences of temperature changes in the wheel and in the area surrounding the wheel on the driving behaviour of the wheel are discussed. The wheel temperature increases when the vehicle is driving and by that also changes the wheel pressure. To take these effects into account, two comparative values for the wheel pressure are created. Ideally, these are close to reality and can therefore predict the actual wheel pressure. The wheel temperature T_w measured at the TB is used to calculate the first reference value for the wheel pressure $P_{comparison,1}$. In addition, average

values are defined for the starting wheel pressure of a wheel at 2,2 bar at of the ambient temperature at 20 °C. The wheel pressure changes by 0,1 bar at a temperature change of 10 K [46], [47], [48]. This corresponds to a pressure change over temperature of 0,01 bar/K. The first reference value for the wheel pressure $P_{comparison,1}$ is calculated in equation (4.29)

$$P_{comparison,1} = 2,2 \text{ bar} + \left[(T_W - 20 \text{ }^\circ\text{C}) * 0,01 \frac{\text{bar}}{\text{K}} \right], \quad (4.29)$$

where $P_{comparison,1}$ – first reference value for the wheel pressure, bar,

T_W – wheel temperature, °C.

The next step is to define a second reference value for the wheel pressure $P_{comparison,2}$ considering the ambient temperature T_A . To do this, the time after which the optimum wheel temperature of around 60 °C is reached during vehicle operation is first calculated [46], [47]. As the wheel is used, it slowly and continuously warms up. Once the operating temperature is reached, as much heat is released into the environment as is generated by driving. It is assumed that at an outside temperature of around 20 °C, this operating temperature of 60 °C is reached after around 30 minutes [46]. This corresponds to a temperature change over time of 1,33 K/min. Furthermore, it is assumed that the wheel has taken up the ambient temperature T_A before starting driving (for example after parking). It is now possible to calculate the time t_M that the wheel needs to reach the operating temperature of 60 °C depending on the measured ambient temperature T_A in equation (4.30)

$$t_M = \frac{60 \text{ }^\circ\text{C} - T_A}{1,33 \frac{\text{K}}{\text{min}}}, \quad (4.30)$$

where t_M – time that the wheel needs to reach the operating temperature of 60 °C, s,

T_A – ambient temperature, °C.

Using this time until the operating temperature t_M is reached, a reference value for the wheel temperature $T_{W,comparison}$ can now be defined in equation (4.31). Ideally, these are identical and it can therefore predict the actual wheel temperature

$$T_{W,comparison} = \begin{cases} T_A + 1,33 \frac{\text{K}}{\text{min}} * t & \text{for } t < t_M \\ 60 \text{ }^\circ\text{C} & \text{for } t \geq t_M \end{cases}. \quad (4.31)$$

where $T_{W,comparison}$ – reference value for the wheel temperature, °C,

t – time, s.

Using this reference value for the wheel temperature $T_{W,comparison}$, which takes into account the ambient temperature and the driving time, the second comparative value for the wheel pressure $P_{comparison,2}$ can now be calculated in equation (4.32)

$$P_{comparison,2} = 2,2 \text{ bar} + \left[(T_{W,comparison} - T_A) * 0,01 \frac{\text{bar}}{\text{K}} \right], \quad (4.32)$$

where $P_{comparison,2}$ – second reference value for the wheel pressure, bar.

To summarise, this extended model can be used to calculate the longitudinal force F_x , the lateral force F_y and the self-aligning torque M_z for three different comparisons (using P , $P_{comparison,1}$ or $P_{comparison,2}$). In addition to the previous influencing factors, the wheel speed v , the wheel shaft angle γ , the wheel centre distance L , the standard acceleration due to earth's gravity g , the wheel temperature T_W and the ambient temperature T_A are also used. Also, in this model the rolling resistance is neglected and it is assumed that c_p and μ are constant and that the pressure is distributed parabolic over a rectangular contact area.

The advanced Simulink model, which simulates the behaviour of the wheel in more detail, also consists of several function blocks. These reflect the logic of the mathematical relationships listed above. An overview of the model is shown in Fig. 4.2.

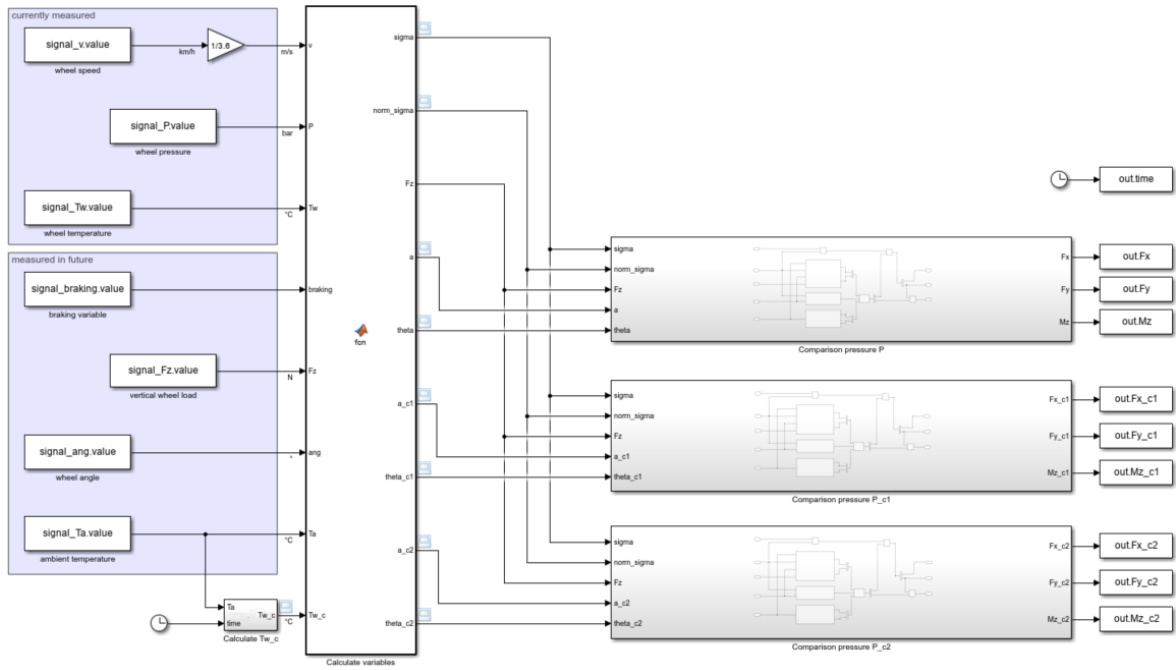


Fig. 4.2: Advanced Simulink model

The shown advanced model also has the first function block "Calculate variables", in which the values for the half-length of the contact area a , the tyre stiffness θ and the theoretical slip quantity σ (as vector $\vec{\sigma}$ and as vector length σ) are calculated based on the formulas described above. However, three different comparison values for the half-length of the contact area and the tyre stiffness are calculated here, each of which takes different influencing factors into account according to the given formulas. The wheel speed v , the wheel pressure P , the wheel temperature T_w , the braking value (0 during driving and 1 during braking), the vertical wheel load F_z , the wheel shaft angle γ , the ambient temperature T_A , the wheel stiffness c_p , the friction coefficient μ , the width of the contact area w and the wheel centre distance L serve as inputs for this.

From this point on, the simulation described in the previous chapter is carried out three times in parallel, each time for differently calculated values for the half-length of the contact area and the tyre stiffness. This results in three different comparison values for the longitudinal force F_x , the lateral force F_y and the self-aligning torque M_z , which can then be plotted and compared with each other at the end.

4.3 Input variables

Within one of the MATLAB codes executed for the simulation, the input parameters for the calculations are defined. These can be changed depending on the application

objective. Examples of changes like this are if the wheels of a different vehicle are to be simulated and the vehicle dimensions and load therefore change, driving on a different surface is to be simulated or the selection between driving and braking is to be changed. The parameters that can be set and their current values are listed in table 4.1.

Table 4.1: Simulation input parameters

Input parameter	Current value
Tire width (m)	0,175
Shaft distance (m)	1,0
Tire pressure (bar)	2,2
Wheel speed (km/h)	10,0
Maximum wheel temperature (°C)	60,0
Ambient temperature (°C)	20,0
Wheel angle (°)	0,0
Vertical wheel load (N)	5000
Stiffness of one thread element (N/m ²)	6000000
Simulation time (s)	3600
Friction coefficient	0,5
Braking variable	0

Particular attention is paid to the friction coefficient, as this parameter cannot be read out or measured easily. Possible methods of how this could be done automatically in the future were presented in chapter 2. Table 4.2 contains a list of some common surface types with the corresponding friction coefficients as an overview for further tests [49], [50].

Table 4.2: Friction coefficient μ of a wheel on different surfaces [49], [50]

Surface type	Wheel rolling/blocked	Friction coefficient μ
Pavement, wet	blocked	0,20
Pavement, dry	blocked	0,50
Beton, wet	rolling	0,30
Beton, dry	rolling	0,50
Ice	rolling	0,05

In future, it should be possible to measure other input parameters automatically and no longer enter them manually. Automatic recording of the frequency transmitted by the frequency converter to the motor and thus the wheel speed is conceivable. Furthermore, the vertical wheel load and the ambient temperature could also be recorded and automatically transmitted in the future (more on this in chapter 7.2).

5 REAL-TIME DATA EXCHANGE

This chapter deals with the connection of the TB and the simulation. The aim is to create a DT by connecting the reality (represented in this project by the data measured on the TB) with its virtual simulation (represented in this project by the simulation in Simulink). The DT becomes more precise and reliable the closer it is to the reality which means the more data from influencing factors are made available to the simulation in real-time. For this thesis, primarily the data of the wheel pressure and the wheel temperature are measured and utilised in order to establish a reliable connection with the help of a MC. If more data flows from other influencing factors are to be established in the future, this connection can be used or further developed.

5.1 Intercepting sensor data

The main sensor used to measure the wheel pressure and wheel temperature is a sensor of a solar powered TPMS of the type TY588-EU2 from "Jansite". This system works by screwing a sensor onto the wheel valve. It can measure the wheel temperature from -20 °C to 85 °C and the wheel pressure from 0 to 3,5 bar with a deviation of $\pm 0,1$ bar. It transmits the data continuously via radio signals at a frequency of 433,92 MHz to a corresponding solar-powered monitor, on which the data can be displayed. [22]

These radio signals are intercepted with the help of a MC. The MC used for this application is a Raspberry Pi 400 from "Raspberry Pi" [39]. To be able to receive radio signals with it, it is connected to a RTL software defined radio (RTL-SDR) dongle [51]. This device is connected to an antenna via a SMA connection and to the MC via an USB port.

Once the device has been successfully installed, the "rtl_433" command can be executed. This is a generic data receiver command with which radio signals from special frequency bands (including the 433,92 MHz band used by the sensor) can be displayed in the terminal. Many decrypting protocols for various sensors are already pre-installed within the command, such as for the Jansite TPMS Model Solar in protocol 180. However, the execution of this protocol does not deliver any data, which is why the signal must be decrypted manually. [52]

5.2 Decrypting sensor data

To check whether data packages are being received by the dongle via the antenna and on which frequency they are, a radio signal is recorded using the "rtl_433" command. In Fig. 5.1 the received frequencies in MHz over the time in ms is shown. As assumed, the signal from the sensor is particularly intense in the frequency range around 433,92 MHz which is marked with a small red line at the left side of the figure. The more yellow the areas are, the stronger the signal was received at the corresponding frequency.

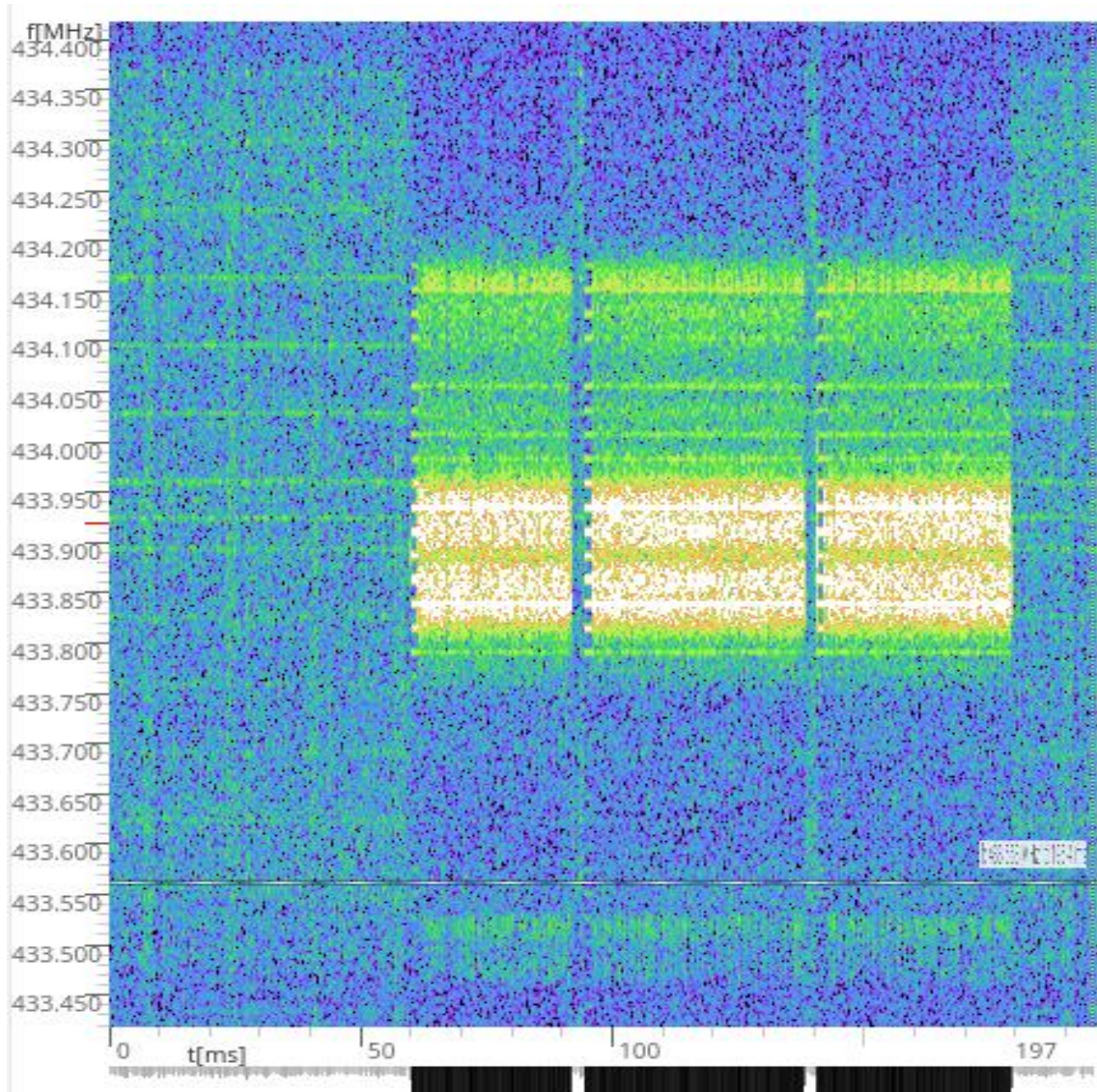


Fig. 5.1: Received radio signal at 433,92 MHz

In order to receive these signals, the "rtl_433" command is executed for the frequency 433,92 Hz, independent from the protocols. New encrypted data packages arrive every time the wheel temperature and wheel pressure change (visible on the corresponding TPMS monitor) and at intervals of six minutes if the parameters do not change. These

packages each consist of a sequence of 128 bits represented in a 32-digit long code in hexadecimal system. The following table 5.1 lists the received codes together with the actual values of wheel pressure and wheel temperature during test runs.

Table 5.1: Received codes for different wheel pressures and temperatures

Wheel pressure (bar)	Wheel temperature (°C)	Received code
1,6	20	{128}5a595a5a655599a569696a5665655a58
1,6	22	{128}a659a659969a65a6a56a56559965a658
1,6	27	{128}96a996a9a5665696aa99a6a5a69596a8
1,6	31	{128}96999699a5565666aaa9a695a6a59698
1,6	35	{128}6569656a56a9a555665995665a556568
1,6	47	{128}9a999a9995565a66a6a9aa959aa59a98
1,6	54	{128}5959595a559996a56a69695666695958
1,7	20	{128}5999599a6569996569a9699665655998 or {128}9999999a5965966a9a9a995a5699998
1,7	21	{128}99699969a5965956aa59a965a5999968
1,7	22	{128}69a969a9aaa9a99559999a6555569a8 or {128}a969a969959a69569a5a59659599a968
1,7	24	{128}6959695a5569a6a55a69995655a56958
1,7	25	{128}99599959a59a56a6aa69a955a5a99958
1,7	29	{128}a999a9996a66696699aa59959565a998 or {128}6959695a5569a6a55a69995655a56958
1,7	31	{128}66695a6a5565a6556559966656a96668
1,7	42	{128}a999a9996a66696699aa59959565a998 or {128}5569556a5aa995559659656669995568
1,8	18	{128}6a596a5a5559a9a559699a55aa996a58
1,8	19	{128}5a595a5a5a9999a5695a9956a5995a58 or {128}a699a699969666669aaa56959655a698
1,8	20	{128}55a955aa69599595959965a666a555a8
1,8	23	{128}a999a9999556696699aa59959555a998
1,8	25	{128}9a599a599a6659a6a969aa559a999a58 or {128}a699a699969666669aaa56959655a698
1,8	27	{128}6aa96aa9a965aa9556999aa5a9a56aa8
1,8	32	{128}a659a659956a65a6a56a56559695a658
1,8	34	{128}5a995a9a56999a6566a96a965a595a98
1,8	37	{128}96a996a99a565696aa99a6a5a5a596a8
1,8	45	{128}69a969a9a655a995599999a5aaa969a8
1,8	49	{128}6aa96aa99a95aa9556999aa5a9a56aa8
1,8	50	{128}65a965a9a969a595659995a656a965a8

A few characteristics stand out. Firstly, each code ends with a hexadecimal "8", which corresponds to the binary sequence of "1000". Furthermore, the rest of all codes consist exclusively of hexadecimal "5", "6", "9" and "a" in different variations, which corresponds to the binary sequences of "0101", "0110", "1001" and "1010". This means that a 0 or 1 cannot be repeated more than twice directly after another in any of the binary codes.

It is also noticeable that two different codes were received at different times for some of the same constellations of wheel pressure and wheel temperature. This can be explained by the fact that the displayed values are rounded and the codes contain more precise data. It is also noticeable that two codes occur twice at different constellations (at 1,7 bar at 24 °C / 29 °C and at 1,8 bar at 19 °C / 25 °C). One explanation for this would be that the information in the code is also dependent on the information in the previous code. Another explanation would be that these are errors, which would be problematic as they cannot be directly identified as such. During the recording of the test series, further errors occurred, but these could always be detected due to different lengths or formats and were also not displayed on the TPMS monitor.

5.3 Data flow to simulation

An important step for establishing a connection from the TB sensors to the simulation is to build up a reliable communication between the intermediate MC and the PC on which the simulation is running. This communication must fulfil several requirements, the two most important of which are reliability and real-time data transmission. Another advantage would be the independence of the location of the two communicators, which means that no physical connection between the MC and the PC would be needed. The two communication options by using an Ethernet cable and by using a database via Wi-Fi are discussed in the following.

The first option to connect the MC to the PC is via an Ethernet cable. This is first connected to the MC and the PC. The MATLAB add-on "MATLAB Support Package for Raspberry Pi Hardware" is then installed on the PC to ensure successful communication [53]. The IP address of the MC must be entered during the setup process. To check whether the connection was successful, the MC will be controlled via the MATLAB terminal. As this works, reliable communication in real-time is possible. However, the disadvantage here is that both sides must be permanently connected to each other via the cable.

The second option is the connection via the use of a database. A database has been created in advance and can receive and upload data (under the link http://api.edlytica.com/upload_robin.php?p=10&t=20&s=1) as well as download and export this data again (under the link http://api.edlytica.com/get_robin.php). The data is transferred to the database using API calls. Currently the three parameters time, wheel pressure and wheel temperature are transferred, but further parameters can be added later if required. To use this communication method, both the MC and the PC must be connected to the internet. The great advantage of this method is that the communication is location independent. This means that the data can be accessed and the simulation operated from any location with internet access. For this reason, it was decided to use this method in the project.

5.4 Simulink data implementation

To be able to use the data from the database in MATLAB and Simulink, the data can be from the database in MATLAB using a code. Within this code, the received data are saved as text and converted into numbers. This numbers can then be saved (and displayed) as a table. Furthermore, the row of values of the table and thus the current values for wheel pressure and wheel temperature are saved into the MATLAB workspace. They are then retrieved from there in Simulink. This means that the current values are always included in the simulation. The code is updating itself once a minute whereby this time can also be changed. When adding further influencing factors that can be measured automatically, the database and the table in MATLAB can simply be expanded accordingly.

6 TESTING

Various tests are planned to be carried out to check how the developed DT behaves and whether it functions as planned. If inaccuracies or malfunctions are detected, the simulation will be adapted accordingly and new tests will then be carried out. By repeating this process, an increasingly accurate DT is created. As many more tests will be carried out later in the project and new influencing factors will be added, this is an ongoing process.

In order to provide an initial overview of whether the setup works as planned and how large the deviations between reality and the simulation are, the first test runs are already planned. These tests are described in this chapter and should also serve as a template for all future tests.

6.1 Setup and execution

The variable influencing factors are first defined to carry out the tests. In the current setup of the TB, these are the wheel speed and the wheel pressure. The wheel speed is adjusted by changing the motor rotational speed by rotating the potentiometer. It can be read from the frequency converter and changed accordingly in the simulation. The wheel pressure is changed by gradually releasing pressure from the wheel by briefly opening the tyre valve. Furthermore, the ambient temperature of the wheel and thus the wheel temperature is influenced by changing the laboratory temperature by closing and opening the laboratory windows. The current wheel pressure and wheel temperature are transmitted by the sensor.

For the test runs, each of these influencing factors is changed in small steps, while the other variables are not changed. This results in a test series for each influencing factor, the results of which will be listed. By not changing the other input parameters it can be guaranteed that the resulting output changes are caused by the changed input parameter. Wheel speed and wheel pressure should be changed in at least ten intermediate steps to get enough data to make the right conclusions. The wheel temperature will only be changed in few intermediate steps, as the ambient temperature (which influences the starting wheel temperature) can only be controllably changed to a small extent with the current TB setup by opening the windows or turning on the heating of the laboratory for example.

6.2 Result recording

A test series is carried out for each adjustable parameter. The outputs of the simulation are noted every time. These are the three comparative values for each of the simulation outputs which are the longitudinal force F_x , the lateral force F_y and the self-aligning torque M_z . These can then be presented as a table or diagram depending on the changed input parameter.

The test procedure for the current setup is as follows. Firstly, the wheel speed is slowly increased using the frequency converter, while the wheel pressure and wheel temperature remain the same. This can be done for example from 0 km/h to 10 km/h in steps of 1 km/h. Then the ambient temperature of the wheel is changed as much as possible, while the wheel pressure and wheel speed remain constant. An attempt should be made to generate as many different temperatures as possible in the laboratory. In the last step, the test series for the wheel pressure is recorded. The temperature remains the same while the wheel pressure is lowered from 2.5 bar to 1.5 bar in 0.1 bar steps for example. After each step the wheel will be accelerated to the same wheel speed.

6.3 Further influencing factors

If other influencing factors are added in the future, further test series can be carried out in which only this variable is changed, while all others remain the same. Examples for this are the angle of the wheel to the underground and the vehicle weight after mounting an underground to the TB. Furthermore, the test series for the different wheel temperatures can be extended if the ambient temperature of the wheel can be better controlled. A plan for this is discussed in the outlook in the next chapter. In addition, further plans are presented there about which influencing factors can be added to the TB in the future and how their entire recording process can be further automated. These additional influencing factors must then also be taken into account accordingly in future tests.

7 RESULTS AND DISCUSSION

The aim of this thesis was to develop a TB for wheel testing including the associated DT. This goal was successfully achieved. This chapter summarises the results and describes what further plans there are for the TB and the DT and what extensions or changes are to be made to them in the future.

7.1 Project results

As part of this project, a TB for wheels was developed, which is located on the TalTech campus. It is driven by an induction motor, which is controlled via a connected frequency converter. The wheel installed on the TB for test purposes can be easily removed or replaced if necessary. The valve on the wheel to be tested in this project is accessible so that the wheel pressure can be changed. By adjusting the height of the steel plates (by screwing the corresponding nuts down or up on the threaded rods) on which the bearings of the wheel shaft are mounted, the tooth belt can be tensioned and the wheel can be set to an angle to a future underground. To operate the TB, the frequency converter must be connected to a 400 V AC supply voltage at 50 Hz.

Furthermore, a simulation was created in Simulink. Based on the mathematical relations, this simulation calculates the longitudinal force, the lateral force and the self-aligning torque of the wheel for three different scenarios. The influencing factors considered in the simulation are the width of the contact area, the wheel pressure, the vertical wheel load, the wheel stiffness, the friction coefficient, the wheel speed, the wheel shaft angle, the wheel centre distance, the wheel temperature and the ambient temperature. Some of these influencing factors are already obtained in real-time from the TB via sensors, while others are currently defined as changeable variables within the simulation.

A sensor screwed onto the wheel valve continuously measures the wheel pressure and wheel temperature and sends this data to a mobile monitor via radio signals. These radio signals can be intercepted using a MC together with a RTL-SDR dongle and an antenna. The data is uploaded to a database in real-time by the MC and downloaded from the PC on which the simulation is carried out. There it is made available for the simulation.

The development of the TB and the DT represent the successful achievement of the objectives of this thesis. With their help, the behaviour of wheels can be realistically

tested under laboratory conditions. From now on the influences of the wheels on the driving behaviour of the autonomous vehicle can also be considered. It is planned that the TB will be further developed and used for educational purposes at the university in the future.

7.2 Further developments of the test bench

The TB was fully constructed and the first tests were planned. Nevertheless, further development and expansion of the TB is possible. On the one hand, this mainly involves adding simulation options for more influencing factors of the wheel, such as the vehicle weight or ambient temperature. On the other hand, various measures can be taken to further increase the safety when using the TB. This is particularly important regarding the planned use of the TB for educational purposes.

The TB was constructed in a way that an underground in the form of a treadmill in the direction of the wheel rotation can later be mounted in the lower area. The wheel can then be pressed against this underground with more or less force by screwing the steel plates down or up, thus simulating different vehicle weights. ISEAUTO has an empty weight m_E of 1250 kg and offers space for a maximum of six people [9]. Assuming an average weight per person m_P of 80 kg and a total tolerance of 15 %, the maximum weight m_{max} can be calculated in equation (7.1). Taking into account the standard acceleration due to earth's gravity g of 9,81 m/s², the force per wheel of the empty vehicle F_E and the following maximum force per wheel F_{max} , which the future underground must be able to withstand, can be calculated in the equations (7.2) and (7.3)

$$m_{max} = (m_E + 6 * m_P) * 1,15 = (1250 \text{ kg} + 6 * 80 \text{ kg}) * 1,15 = 1989,5 \text{ kg} , \quad (7.1)$$

where m_{max} – maximum weight, kg,

m_E – empty weight, kg,

m_P – average weight of a person, kg,

$$F_E = \frac{m_E}{4} * g = \frac{1250 \text{ kg}}{4} * 9,81 \frac{\text{m}}{\text{s}^2} = 3065,6 \text{ N} , \quad (7.2)$$

where F_E – force per wheel of the empty vehicle, N,

$$F_{max} = \frac{m_{max}}{4} * g = \frac{1989,5 \text{ kg}}{4} * 9,81 \frac{\text{m}}{\text{s}^2} = 4879,3 \text{ N}, \quad (7.3)$$

where F_{max} – maximum force per wheel, N.

The bearings, as one of the most stressed components, support these forces [27], [28]. Furthermore, the formula provided by the profile manufacturer is used in equation (7.4) to ensure that this maximum force flow does not stress the for this purpose installed aluminium profiles beyond the defined limit of the maximum deflection f_{max} of 0,5 mm [29]. The two loaded profiles have a respective length of 0,8 m, a cross-section of 90 x 90 mm and thus an area moment of inertia of 230 kg*m² [29]

$$f_{max} = \frac{F_{max} * L^3}{E * I * 48 * 10^4} = \frac{\frac{4979.3 \text{ N}}{2} * (800 \text{ mm})^3}{70000 \frac{\text{N}}{\text{mm}^2} * 230 \text{ cm}^4 * 48 * 10^4} = 0,165 \text{ mm}. \quad (7.4)$$

The profiles bend less than 0,5 mm even under maximum load. By this, all components already installed fulfil the requirements. An appropriate underground can therefore be installed in future together with a measuring system for the exerted load. In order to simulate the reality as good as possible, it was decided to use a flat underground such as a treadmill rather than a rotating drum. This treadmill must support weights of up to 500 kg in order to be able to simulate the maximum vehicle weight per wheel. It must also be ensured that this load is only distributed over the small contact area of the wheel on the underground. The selected treadmill must fulfil these requirements.

Furthermore, it would be conceivable that after the addition of an underground, the friction coefficient arising between the tyre and the surface could be recorded automatically using one of the methods presented in the state of the art [23], [24]. Like that it would be no longer necessary to be change this coefficient manually in the simulation.

As a further safety feature, it would be possible to install plexiglass panes around the TB. They can prevent improper contact and avoid that parts are thrown out of the TB in the event of a malfunction. Another advantage of this is that it would be possible to change the temperature inside this housing to a certain extend for a possible simulation of the wheel's ambient temperature. A heating and cooling system for the interior of the plexiglass housing could be installed for this purpose. However, it should be noted that the motor of the TB, which would also be inside the housing, has a maximum permissible ambient temperature of 40 °C [54]. This would therefore be the maximum ambient temperature of the wheel that can be simulated.

To determine the extent to which the aluminium profile system, as an important and heavily loaded basic structure element of the TB, can withstand these temperature changes, its material must be analysed. The aluminium alloy EN-AW-6063 T66 used has a thermal expansion coefficient α of $23,4 * 10^{-6} K^{-1}$ [55]. If a minimum temperature T_{min} of $-10\text{ }^{\circ}C$ and a maximum temperature T_{max} of $40\text{ }^{\circ}C$ due to the motor operation limits is considered, the maximum material expansion ΔL can be calculated in the equations (7.5) and (7.6)

$$\Delta L_{1m} = \alpha * (T_{max} - T_{min}) = 0,0234 \frac{mm}{K} * (40\text{ }^{\circ}C - (-10\text{ }^{\circ}C)) = 1,17mm, \quad (7.5)$$

where ΔL_{1m} – maximum material expansion per 1m, m,

T_{max} – maximum temperature, $^{\circ}C$,

T_{min} – minimum temperature, $^{\circ}C$,

$$\Delta L_{1,18m} = \Delta L_{1m} * \frac{1,18\text{ m}}{1\text{ m}} = 1,17\text{ mm} * 1,18 = 1,38\text{ mm}, \quad (7.6)$$

where $\Delta L_{1,18m}$ – maximum material expansion per 1,18m, m.

The maximum material expansion of the aluminium profiles, which would take place at the assumed maximum change of the ambient temperature, is 1,17 mm per meter in each direction. This corresponds to 1,38 mm in length of the longest mounted profile of 1,18 m.

7.3 Connection with other digital twin models

The developed DT can calculate the impact of the wheels on the driving behaviour of the entire vehicle based on data collected at the TB. To further utilise these obtained data, it makes sense to connect this DT with other DTs and thus make predictions about multiple components or the entire vehicle. More complex DTs are more accurate because more data is included.

On the one hand, the inputs of the wheel DT can be controlled. An example of this that has already been implemented is the ability to control the wheel speed externally. A voltage between $+3,3\text{ V}$ and 0 V can be applied via the two analogue inputs AI1- and AI1+ of the frequency converter, which controls the speed and direction of the wheel rotation. With a voltage between $3,3\text{ V}$ and $1,65\text{ V}$, the wheel rotates forwards

proportional to the voltage, with a voltage of exactly 1,65 V it stops and with a voltage between 1,65 V and 0 V the wheel rotates backwards anti-proportional to the voltage. This voltage control is currently performed with a potentiometer, but can also be controlled by an external MC. This provides a potential interface for communication with other DTs.

On the other hand, the outputs calculated in the simulation can be used further. It is conceivable that the calculated values for the longitudinal force, the lateral force and the self-aligning torque of the wheel are exported from Simulink and made available for communication with the other DTs and their further calculations.

The way in which this communication between the DTs as well as between the TB and the simulation can take place is by using ROS2. To enable reliable cooperation between the various components such as sensors and motors, a MC is used as an intermediate bridge. It can send and receive data via ROS2 using micro-ROS. The hardware of the DTs (the wheel TB in this case) can then be controlled by the system via the control of their analogue and digital inputs.

An example of a DT with which the DT presented in this thesis could communicate is the DT of a propulsion drive of an autonomous electric vehicle, which was presented in [8] and is also based on ISEAUTO. This has various physical models of different components of the powertrain such as motors and batteries and various sensors on a TB. The virtual simulation is carried out using a 3D model of ISEAUTO. Influencing factors such as the road conditions, the vehicle mass and the speed can also be set manually in this simulation. [8]

8 SUMMARY

Research of autonomous electric vehicles has developed rapidly in recent years. One aspect that has received little attention so far is the influence of the wheels on the driving behaviour of the vehicles. To change that, some TBs and DTs have already been developed regarding this topic, but these have mostly focussed either on a specific aspect of the wheel or on the vehicle's entire powertrain.

In the context of this thesis, a TB was designed and constructed on the TalTech campus on which various influencing factors of wheels can be simulated and adjusted under laboratory conditions. The resulting changes in the behaviour of the wheel are measured by sensors and transmitted via radio signal. By using an MC with a connected antenna and a database, the data can be intercepted and transferred in real-time to a simulation of the wheel in Simulink. By using a database for the data flow, the simulation can be carried out location-independently of the TB. The simulation calculates the expected forces on the wheel based on mathematical relations. These relations were explained in detail in the thesis.

So far, the wheel pressure and wheel temperature are transferred from the wheel on the TB to the simulation and influencing factors such as wheel speed, wheel pressure and wheel angle can be adjusted on the TB. In the future, it is possible to take other influencing factors such as the load of the vehicle or the friction coefficient between the wheel and the road into account by adding further components to the TB such as a suitable underground. The DT can also be extended accordingly by adding further sensors and receive more real-time data like this.

The development of a TB together with the associated DT was successful. Nevertheless, it should be mentioned that a DT becomes more accurate and reliable through continuous optimisation and expansion. The DT presented in this thesis has great potential for improvement. Some of the possible extensions were discussed in detail and recommended in the thesis.

9 KOKKUVÕTE

Autonoomsete elektrisõidukite alased teadusuuringud on viimastel aastatel kiiresti arenenud. Üks aspekt, millele on seni vähe tähelepanu pööratud, on olnud rataste mõju sõidukite sõiduomadustele. Sel teemal on juba välja töötatud katsestendid ja digitaalsed kaksikud, kuid need on enamasti keskendunud kas ratta konkreetsele aspektile või kogu sõiduki jõuülekandele.

Käesoleva lõputöö raames projekteeriti ja rajati TalTechi ülikoolilinnakusse katsestend, kus saab simuleerida ja reguleerida erinevaid rattaid mõjutavaid tegureid laboritingimustes. Sellest tulenevaid muutusi ratta käitumises mõõdetakse anduritega ja edastatakse raadiosignaali kaudu. Ühendatud antenniga mikrokontrolleri ja andmebaasi abil oli võimalik andmeid kinni pidada ja edastada need reaajas Simulinkis toimuvale ratta simulatsioonile. Kasutades andmevoo jaoks andmebaasi, saab simulatsiooni teostada katsepinkidest sõltumatult. Simulatsioon arvutab matemaatiliste seoste alusel välja rattale mõjuvad eeldatavad jõud. Neid seoseid selgitati üksikasjalikult lõputöös.

Praegu kantakse ratta rõhk ja ratta temperatuur katsestendil olevast rattast üle simulatsiooni ning selliseid mõjutegureid nagu kiirus, rehvirõhk ja ratta nurk saab katsestendil seadistada. Tulevikus peaks olema võimalik arvesse võtta ka muid mõjutavaid tegureid, nagu sõiduki koormus või hõõrdetegur, lisades täiendavaid komponente, näiteks sobiva pinna. Samuti saab digitaalset kaksikut vastavalt laiendada, lisades täiendavaid andureid.

Katsestendi ja sellega seotud digitaalse kaksiku väljatöötamine oli seega edukas. Siiski tuleb märkida, et digitaalne kaksik muutub pideva optimeerimise ja laiendamise kaudu täpsemaks ja usaldusväärsemaks. Siin esitatud digitaalsel kaksikudelil on suur arengupotentsiaal. Mõned võimalikud laiendused on käesolevas töös üksikasjalikult käsitletud ja soovitatud.

LIST OF FIGURES

Fig. 2.1: TB for tyre-road interaction during braking [10]	15
Fig. 2.2: TB diagram for all-electric ABS [11]	16
Fig. 2.3: Illustrative diagram of a powertrain TB [15].....	17
Fig. 2.4: Structure of a DT [7].....	18
Fig. 3.1: TB 3D model	23
Fig. 3.2: Wheel TB	29
Fig. 4.1: Simulink model [42]	35
Fig. 4.2: Advanced Simulink model	41
Fig. 5.1: Received radio signal at 433,92 MHz	45

LIST OF TABLES

Table 4.1: Simulation input parameters	42
Table 4.2: Friction coefficient μ of a wheel on different surfaces [49], [50]	42
Table 5.1: Received codes for different wheel pressures and temperatures	46

LIST OF REFERENCES

- [1] Tallinna Tehnikaülikool, "Tallinna Tehnikaülikool." Accessed: Nov. 20, 2023. [Online]. Available: <https://taltech.ee/>
- [2] Tallinna Tehnikaülikool, "Development of a test bench for wheel testing including the associated digital twin." Accessed: Nov. 21, 2023. [Online]. Available: <https://taltech.ee/en/coophost>
- [3] Tallinna Tehnikaülikool, "Mechatronics and Autonomous Systems Research Group." Accessed: Nov. 20, 2023. [Online]. Available: <https://taltech.ee/en/mechatronics-and-autonomous-systems>
- [4] R. Köppe, *Master's thesis - Topic: Development of a test bench for wheels of a propulsion drive system including the associated digital twin.* 2024.
- [5] etis.ee, "R&D project: Development of a test bench for wheel testing including the associated digital twin." Accessed: Nov. 21, 2023. [Online]. Available: <https://www.etis.ee/Portal/Projects/Display/ad7dbb08-26be-4a31-b684-e5e8126b4b5e>
- [6] etis.ee, "R&D project: Digital twin for propulsion drive of autonomous electric vehicle." Accessed: Nov. 20, 2023. [Online]. Available: https://www.etis.ee/Portal/Projects/Display/72b66c74-e911-49c3-ac6a-6716f9e72ba5?tabId=tab_GeneralData&lang=ENG
- [7] A. Rassolkin, T. Vaimann, A. Kallaste, and V. Kuts, "Digital twin for propulsion drive of autonomous electric vehicle," *2019 IEEE 60th Annual International Scientific Conference on Power and Electrical Engineering of Riga Technical University, RTUCON 2019 - Proceedings*, Oct. 2019, doi: 10.1109/RTUCON48111.2019.8982326.
- [8] A. Rassolkin, V. Rjabtsikov, T. Vaimann, A. Kallaste, and V. Kuts, "Concept of the Test Bench for Electrical Vehicle Propulsion Drive Data Acquisition," *2020 11th International Conference on Electrical Power Drive Systems, ICEPDS 2020 - Proceedings*, Oct. 2020, doi: 10.1109/ICEPDS47235.2020.9249078.
- [9] Tallinna Tehnikaülikool, "Estonian first level 4 self-driving vehicle – ISEAUTO." Accessed: Nov. 23, 2023. [Online]. Available: <https://autolab.taltech.ee/portfolio/iseauto/>
- [10] M. Vignati, D. Tarsitano, and E. Sabbioni, "Modeling of a single wheel test bench for blended electric and hydraulic brake testing," *2021 AEIT International Conference on Electrical and Electronic Technologies for Automotive, AEIT AUTOMOTIVE 2021*, 2021, doi: 10.23919/AEITAUTOMOTIVE52815.2021.9662921.

- [11] X. Xue *et al.*, "Design, Analysis and Application of Single-Wheel Test Bench for All-Electric Antilock Braking System in Electric Vehicles," *Energies* 2021, Vol. 14, Page 1294, vol. 14, no. 5, p. 1294, Feb. 2021, doi: 10.3390/EN14051294.
- [12] J. Kres, A. Morgado-Estevez, F. Perez-Pena, K. Schmidt, and H. P. Hebert, "Development of single-Axis Wheel Speed Sensor HiL Test Bench for Vehicle Velocity Control," *HORA 2021 - 3rd International Congress on Human-Computer Interaction, Optimization and Robotic Applications, Proceedings*, Jun. 2021, doi: 10.1109/HORA52670.2021.9461305.
- [13] H. Ye, S. Ma, Y. Liu, Y. Jin, and L. Zhu, "Design of test bench system for hybrid driving system," *IEEE Transportation Electrification Conference and Expo, ITEC Asia-Pacific 2014 - Conference Proceedings*, Oct. 2014, doi: 10.1109/ITEC-AP.2014.6940923.
- [14] M. Gerard, "Tests and comparison of two electrical powertrain systems by vehicle simulation test bench and vehicle modeling," *2012 IEEE Vehicle Power and Propulsion Conference, VPPC 2012*, pp. 826–829, 2012, doi: 10.1109/VPPC.2012.6422732.
- [15] P. M. Fonte, P. Almeida, R. Luis, R. Pereira, and M. Chaves, "Powertrain Test Bench System," *2019 Electric Vehicles International Conference, EV 2019*, Oct. 2019, doi: 10.1109/EV.2019.8892925.
- [16] V. Rjabtsikov *et al.*, "Digital Twin Service Unit Development for an EV Induction Motor Fault Detection," *2023 IEEE International Electric Machines and Drives Conference, IEMDC 2023*, 2023, doi: 10.1109/IEMDC55163.2023.10239085.
- [17] M. S. Elbakry, A. M. Mahmoud, S. E. Hassan, and T. Ismail, "Digital Twin Simulations for Connected and Automated Vehicles: A Comprehensive Study," *ICEEM 2023 - 3rd IEEE International Conference on Electronic Engineering*, 2023, doi: 10.1109/ICEEM58740.2023.10319570.
- [18] S. Venturini, C. Rosso, and M. Velardocchia, "An automotive steel wheel digital twin for failure identification under accelerated fatigue tests," *Eng Fail Anal*, vol. 158, p. 107979, Apr. 2024, doi: 10.1016/J.ENGFAILANAL.2024.107979.
- [19] S. Gryś, "An Experimental Test Bench for the Tire Pressure Monitoring System – Discussion of Measurement and Communication Issues," *International Journal of Electronics and Telecommunications*, 2019, doi: 10.24425/123565.
- [20] Tomorrow's Technician Staff, "Porsche Tech Tip: TPMS." Accessed: Apr. 24, 2024. [Online]. Available: <https://www.tomorrowstechnician.com/porsche-tech-tip-tpms/>
- [21] European Parliament, *REGULATION (EC) No 661/2009 OF THE EUROPEAN PARLIAMENT AND OF THE COUNCIL of 13 July 2009*. 2009.

- [22] Jansite, "Jansite Original Solar TPMS Car Tire Pressure Best Alarm Monitor System." Accessed: Nov. 17, 2023. [Online]. Available: <https://jansite.com/products/jansite-original-solar-tpms-car-tire-pressure/>
- [23] R. Matsuzaki, K. Kamai, and R. Seki, "Intelligent tires for identifying coefficient of friction of tire/road contact surfaces using three-axis accelerometer," *Smart Mater Struct*, vol. 24, no. 2, p. 025010, Dec. 2014, doi: 10.1088/0964-1726/24/2/025010.
- [24] F. Holzmann, M. Bellino, R. Siegart, and H. Bubb, "Predictive estimation of the road-tire friction coefficient," *Proceedings of the IEEE International Conference on Control Applications*, pp. 885–890, 2006, doi: 10.1109/CACSD-CCA-ISIC.2006.4776762.
- [25] Dassault Systèmes SolidWorks Corporation, "SOLIDWORKS 3D CAD." Accessed: Nov. 21, 2023. [Online]. Available: <https://www.solidworks.com/product/solidworks-3d-cad>
- [26] MiniTec Framing Systems LLC, "CAD." Accessed: Nov. 21, 2023. [Online]. Available: https://www.minitecframing.com/MiniTec_CAD_File_Location.html
- [27] AB SKF (publ.), *SKF UCP 205/H Specification*. 2023. Accessed: Mar. 29, 2023. [Online]. Available: <https://www.skf.com/id/products/mounted-bearings/ball-bearing-units/pillow-block-ball-bearing-units/productid-UCP%20205%2FH>
- [28] AB SKF (publ.), *SKF UCP 206/H Specification*. 2023. Accessed: Mar. 29, 2023. [Online]. Available: <https://www.skf.com/id/products/mounted-bearings/ball-bearing-units/pillow-block-ball-bearing-units/productid-UCP%20206%2FH>
- [29] MiniTec GmbH & Co. KG, *MiniTec PROFILE SYSTEM Product catalog*, 95.3010/3. 2019. Accessed: Apr. 17, 2023. [Online]. Available: https://www.minitecautomation.com/fileadmin/user_upload/downloads/downloads_en/HK2019_ENG_interaktiv_komprimiert.pdf
- [30] MiniTec Solutions, "21.0978/0 - Angle 90 (with hardware)." Accessed: Nov. 17, 2023. [Online]. Available: <https://www.minitecsolutions.com/product/21-0978-0/>
- [31] K-rauta, "Varras Haushalt DIN 975, 1000 mm x 30 mm tsingitud." Accessed: Nov. 17, 2023. [Online]. Available: <https://www.k-rauta.ee/p/varras-haushalt-din-975-1000-mm-x-30-mm-tsingitud/2wtf>
- [32] Corm OÜ, "Teraslehe S355 lõikamine - metall24.ee." Accessed: Nov. 17, 2023. [Online]. Available: <https://www.metall24.ee/tooted/teraslehe-s355-loikamine>
- [33] MÄDLER GmbH, "Taper-Spannbuchse 1108 Bohrung 19mm." Accessed: Nov. 17, 2023. [Online]. Available: <https://www.maedler.de/Article/62250219>

- [34] MÄDLER GmbH, "HTD-Zahnriemenrad aus Stahl Profil 8M 24 Zähne für Riemenbreite 20mm für Taper-Spannbuchse 1108." Accessed: Nov. 17, 2023. [Online]. Available: <https://www.maedler.de/Article/17477112>
- [35] Alas-Kuul AS, "Koonuspuks (62250214) 1108 d=19mm." Accessed: Nov. 17, 2023. [Online]. Available: <https://www.alas-kuul.ee/koonuspuks-62250219-1108-d-19mm-tl-1108-19>
- [36] Alas-Kuul AS, "Hammasrihma ratas (17477112), HTD 8M rihmale laiusega 20mm. z=24, koonuspuksile 1108, teras." Accessed: Nov. 17, 2023. [Online]. Available: <https://www.alas-kuul.ee/hammasrihma-ratas-17477112-htd-8m-rihmale-laiusega-20mm-z-24-koonuspuksile-1108-teras-bl-24-8m-20-1108-chia>
- [37] MÄDLER GmbH, "Zahnriemen Profil HTD 8M, Breite 20 mm." Accessed: Nov. 17, 2023. [Online]. Available: <https://www.maedler.de/product/1643/1616/970/zahnriemen-profil-htd-8m-breite-20-mm>
- [38] Alas-Kuul AS, "Hammasrihma ratas (17414600), HTD 8M rihmale laiusega 20mm. z=112, töötlemata ava, malm." Accessed: Nov. 17, 2023. [Online]. Available: <https://www.alas-kuul.ee/hammasrihma-ratas-17414600-htd-8m-rihmale-laiusega-20mm-z-112-tootlemata-ava-malm-112-8m-20-fb-mad>
- [39] Raspberry Pi, "Raspberry Pi 400." Accessed: Nov. 17, 2023. [Online]. Available: <https://www.raspberrypi.com/products/raspberry-pi-400/>
- [40] DIGIPURK OÜ, "433 Mhz RF Transmitter and Receiver." Accessed: Nov. 17, 2023. [Online]. Available: <https://digipurk.ee/toode/433-mhz-rf-transmitter-and-receiver/>
- [41] The MathWorks Inc., "MATLAB." Accessed: Dec. 18, 2023. [Online]. Available: <https://de.mathworks.com/products/matlab.html>
- [42] N. Duphil and B. Granouillac, *Tyre Matlab Model*. 2022.
- [43] H. J. Schlichting, "Zur Gleichgewichtsproblematik beim Fahrradfahren".
- [44] The Autopian, "Why Some Cars Have A Bigger Turning Radius Than Others." Accessed: Apr. 18, 2024. [Online]. Available: <https://www.theautopian.com/the-engineering-behind-why-some-cars-can-turn-tighter-than-others/>
- [45] H. B. Pacejka, "Tire Steady-State and Dynamic Test Facilities," *Tire and Vehicle Dynamics*, pp. 567–576, 2012, doi: 10.1016/B978-0-08-097016-5.00012-7.
- [46] Oponeo.de, "Reifentemperatur." Accessed: Apr. 18, 2024. [Online]. Available: <https://www.oponeo.de/blog/reifentemperatur>
- [47] InReifen.de, "Spielt die Reifentemperatur eine Rolle? Wann sollte ich Sommerreifen durch Winterreifen ersetzen?" Accessed: Apr. 18, 2024. [Online].

- Available: <https://www.inreifen.de/akt,0,365/spielt-die-reifentemperatur-eine-rolle--wann-sollte-ich-sommerreifen-durch-winterreifen-ersetzen--.html>
- [48] Aircom, "Wie wirkt sich das Wetter auf den Reifendruck aus?" Accessed: Apr. 18, 2024. [Online]. Available: <https://aircom.ag/de/wie-wirkt-sich-das-wetter-auf-den-reifendruck-aus/>
- [49] H. 1923-2021 Kuchling, "Taschenbuch der Physik", Accessed: Apr. 18, 2024. [Online]. Available: <https://search.worldcat.org/title/918499560>
- [50] Anton Schweizer, "Gleitreibwerte von verschiedenen Materialien." Accessed: May 06, 2024. [Online]. Available: https://www.schweizer-fn.de/stoff/reibwerte/reibwerte_gleitreibung.php
- [51] rtl-sdr.com, "About RTL-SDR." Accessed: May 07, 2024. [Online]. Available: <https://www.rtl-sdr.com/about-rtl-sdr/>
- [52] "rtl_433." Accessed: May 07, 2024. [Online]. Available: https://triq.org/rtl_433/
- [53] The MathWorks Inc., "MATLAB Support Package for Raspberry Pi Hardware." Accessed: Mar. 24, 2024. [Online]. Available: <https://de.mathworks.com/matlabcentral/fileexchange/45145-matlab-support-package-for-raspberry-pi-hardware>
- [54] Lenze SE, *Lenze MCS Synchronous Servo Motors*.
- [55] Kloeckner Metals Germany GmbH, "EN AW 6060 Datenblatt: Eigenschaften, Anwendungsgebiete." Accessed: Dec. 09, 2023. [Online]. Available: <https://facts.kloeckner.de/werkstoffe/aluminium/3-3206/>

APPENDICES

Appendix 1: Command to receive sensor radio signals

```
rtl_433 -f 433.92M -s 1000k -R 0 - X  
'n=name,m=OOK_PCM,s=50,l=50,r=150,preamble=aaa9
```

Appendix 2: MATLAB code for receiving sensor data from database

```
while true % Loop for automated updating

%% Get data from database
data = webread("http://api.edlytica.com/get_robin.php"); % Get data from
database
json_string = data; % Change data type to JSON string
data_struct = jsondecode(['[', strrep(json_string, '{}', '{},{'}, '], ']); %
Decode JSON string to MATLAB structure

%% Plot data as table
data_table = struct2table(data_struct); % Create table
data_table = array2table(str2double(table2array(data_table))); % Change text
to numbers
data_table.Properties.VariableNames = {'ID', 'Wheel pressure (bar)', 'Wheel
temperature (°C)', 'Time (min)'}; % Define column names
disp(data_table); % Plot table (can be turned off if table should not be
displayed)

%% Save data to workspace as double
current_row = size(data_table, 1);
current_data_row = data_table(current_row, :);
current_id = current_data_row.ID;
current_pressure = current_data_row('Wheel pressure (bar)');
current_temperature = current_data_row('Wheel temperature (°C)');
current_time = current_data_row('Time (min)');

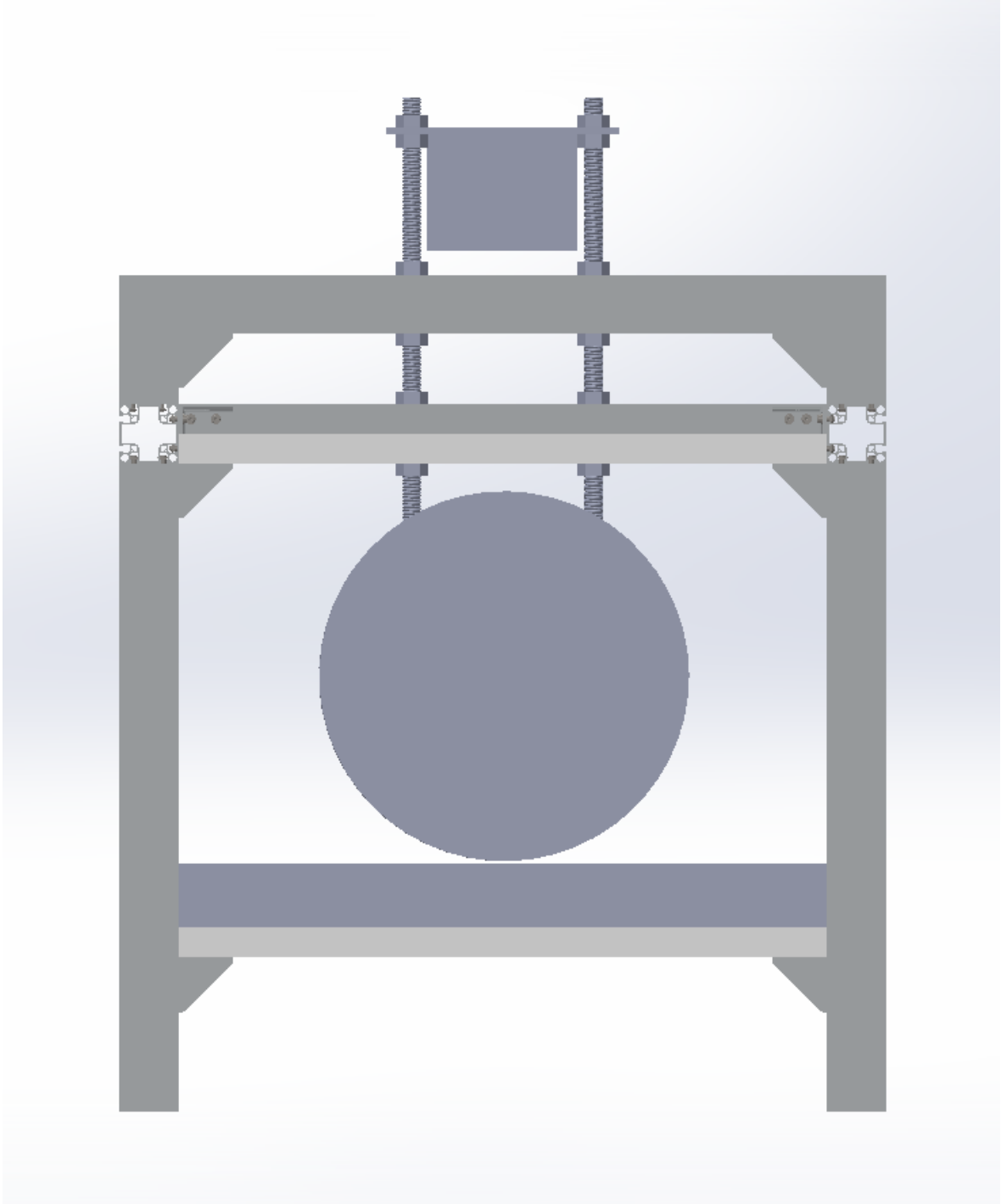
assignin('base', 'current_id', current_id);
assignin('base', 'current_pressure', current_pressure);
assignin('base', 'current_temperature', current_temperature);
assignin('base', 'current_time', current_time);

%% Repeat code and update table automatically
pause(60); % Repeating time in seconds

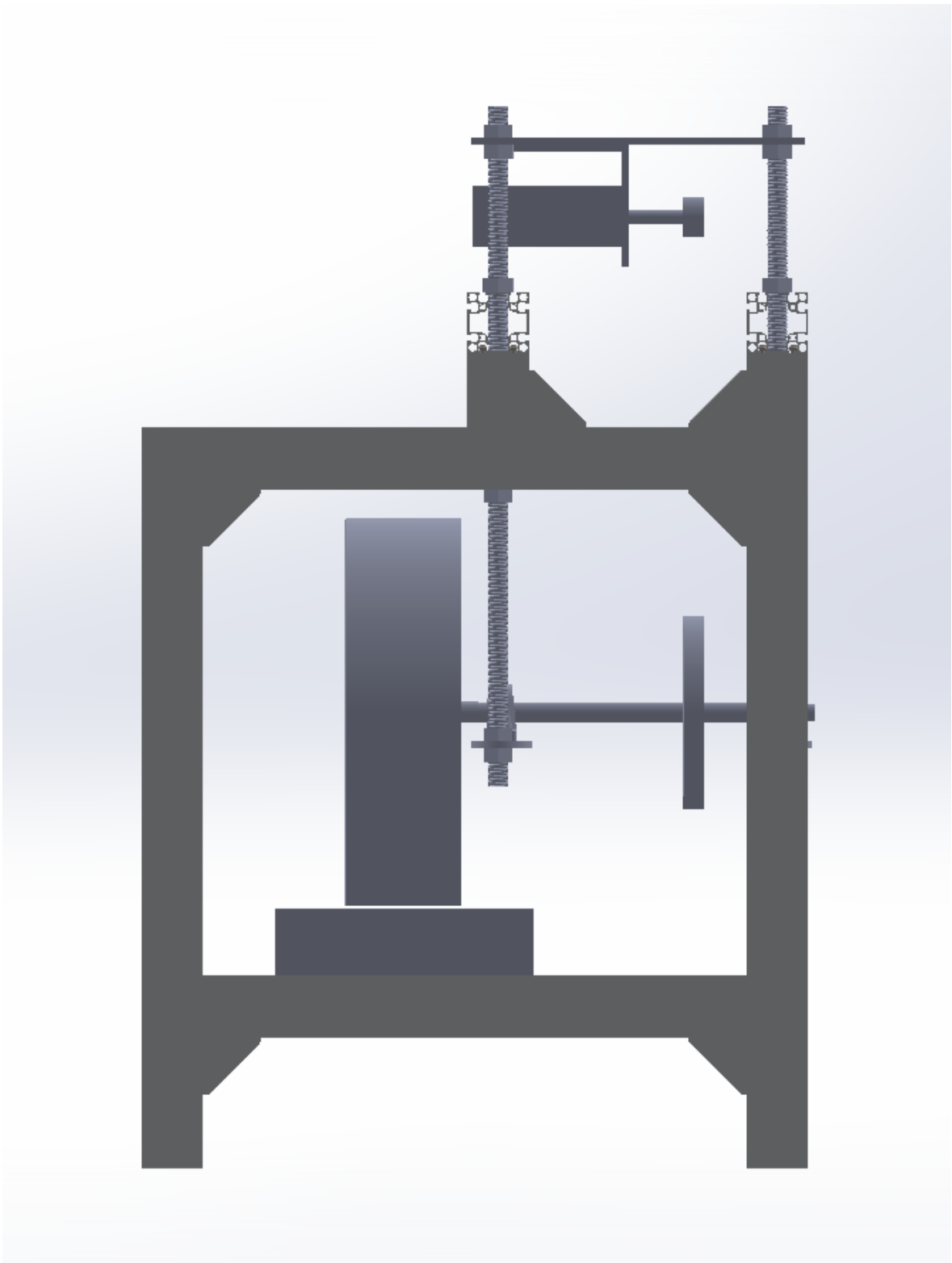
end
```

GRAPHICAL MATERIAL

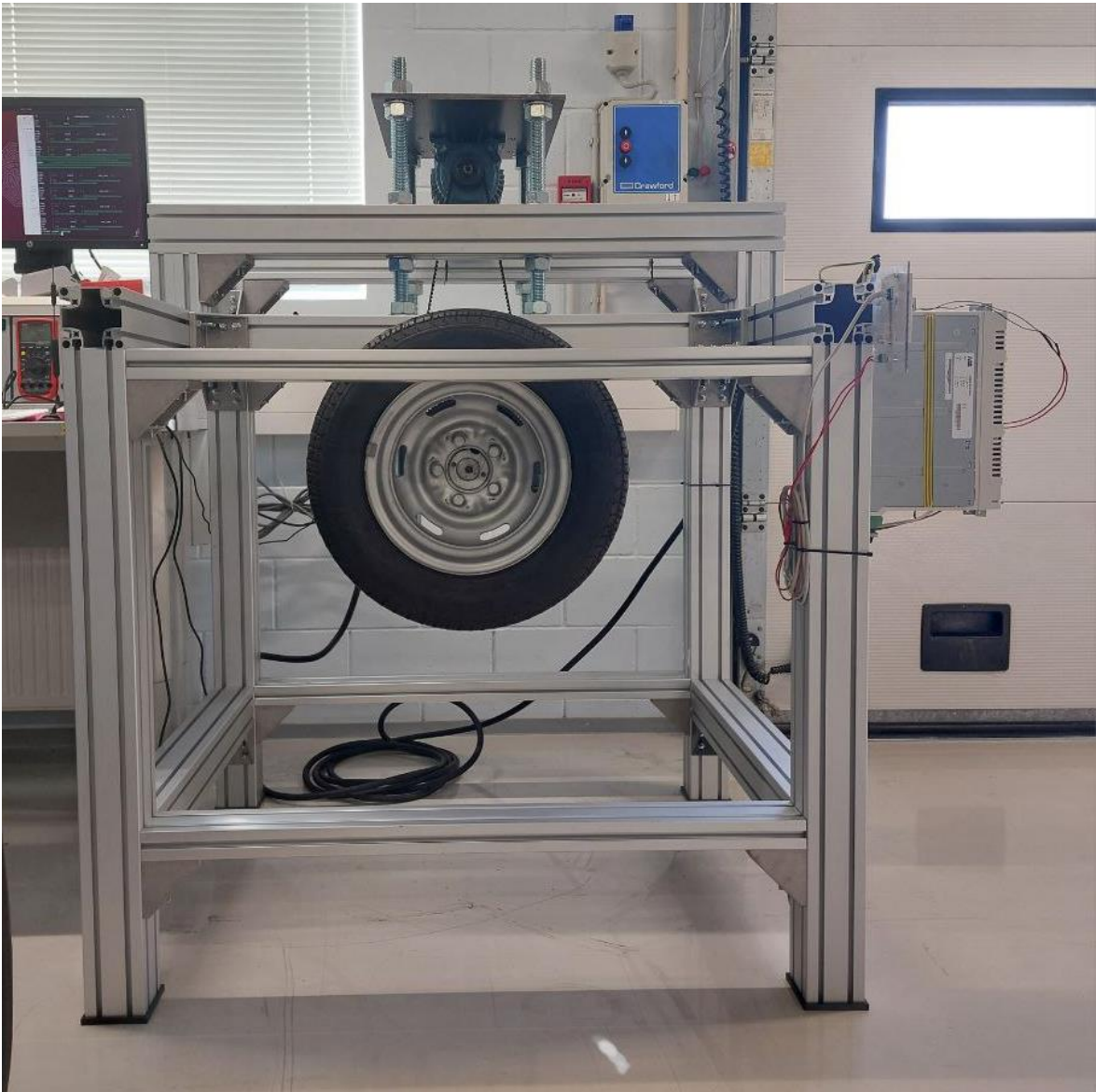
Graphic material 1: Front view of the 3D model



Graphic material 2: Side view of the 3D model



Graphic material 3: Front view of the test bench



Graphic material 4: Side view of the test bench

